Grafene e "suoi derivati"

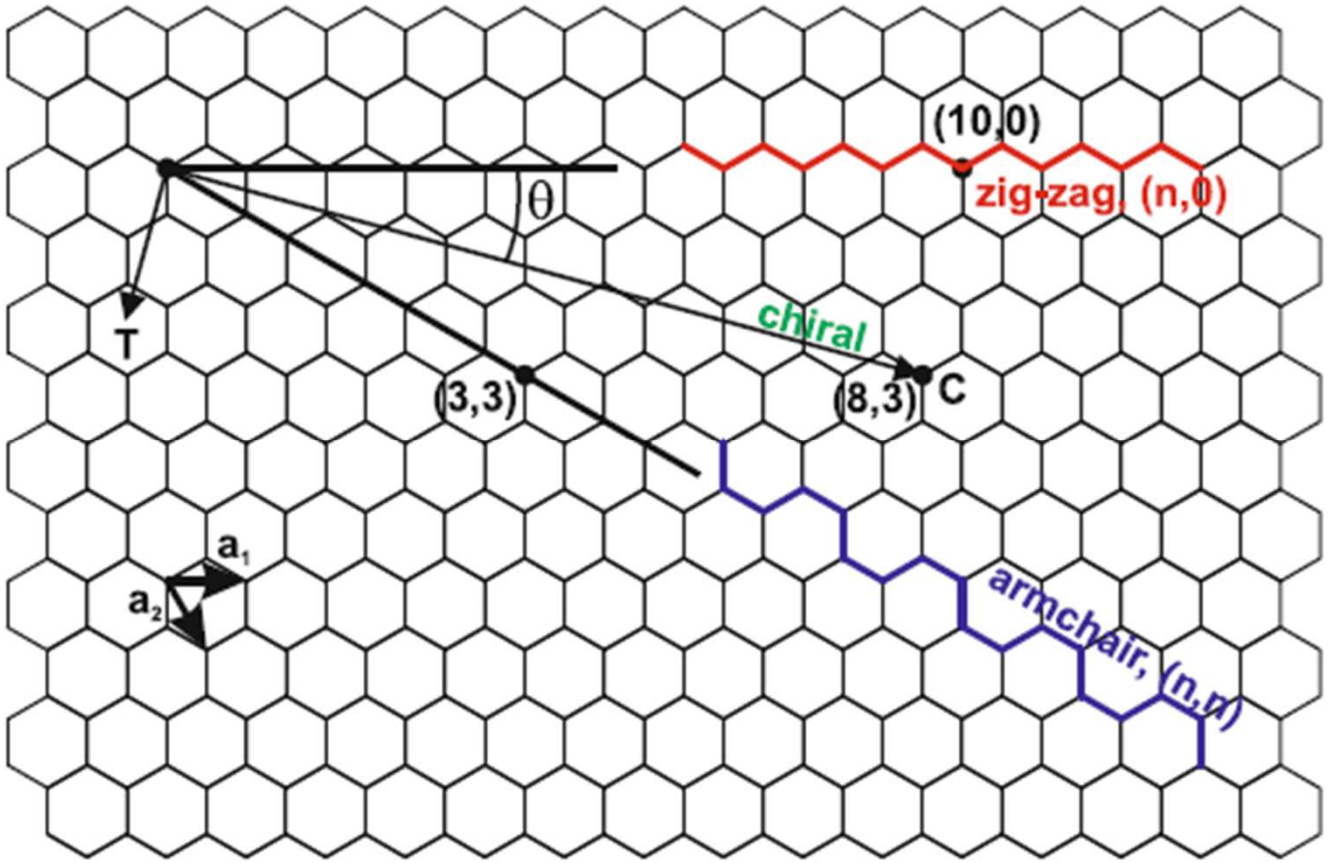

Sommario

- Proprieta' strutturali ed elettroniche
- Preparativa e proprietà microscopiche
- Derivati

- Proprieta' strutturali ed elettroniche
- Preparativa e proprietà microscopiche
- Derivati

Il GRAFENE

Birthdate 2004

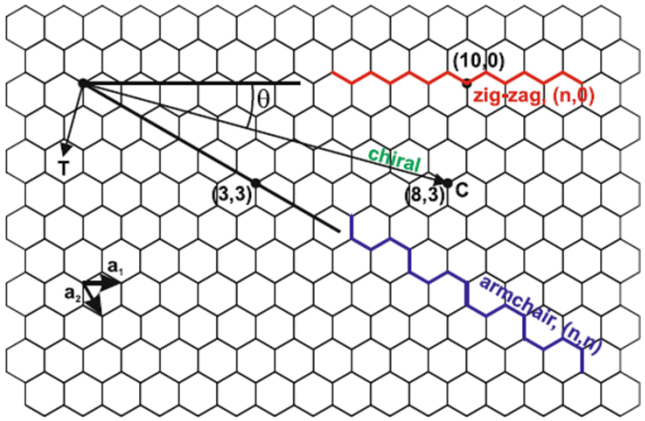

Fig. 17.1. Schematic atomic arrangement in graphene; the C–C bond length is $d_{C-C} = 0.142\,\text{nm}$. Several vectors for making carbon nanotubes (cf. Sect. 17.2) are shown

GRAPHENE: MATERIALS IN THE FLATLAND

Nobel Lecture, December 8, 2010

by

KONSTANTIN S. NOVOSELOV

School of Physics and Astronomy, The University of Manchester, Oxford Road, Manchester M13 9PL, UK.

The major draw to people in the field, though, is graphene's unique properties, each of which seems to be superior to its rivals. This material is the first 2D atomic crystal ever known to us [3]; the thinnest object ever obtained; the world's strongest material [12]; its charge carriers are massless Dirac fermions [7, 13–14]; it is extremely electrically [15] and thermally [16] conductive; very elastic; and impermeable to any molecules [17] – the list goes on. Even a simple inventory of graphene's superlative qualities would require several pages, and new entries are being added on a monthly basis.

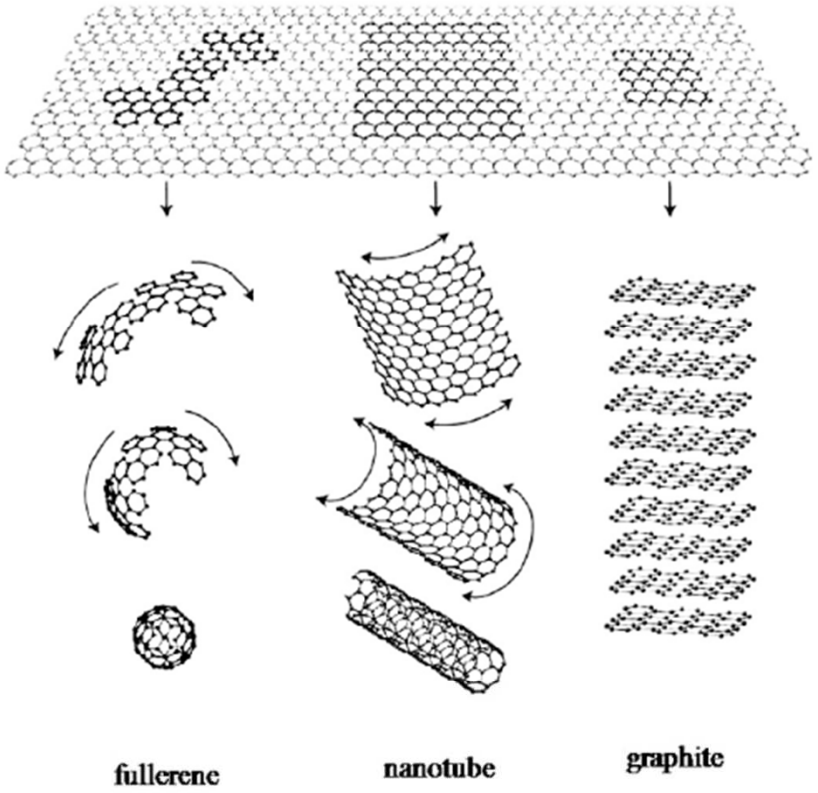

Fig. 1. Graphene: mother of all graphitic forms (From reference 1).

MATERIALS THAT SHOULD NOT EXIST

More than 70 years ago, Landau and Peierls argued that strictly 2D crystals were thermodynamically unstable and could not exist[11,12]. Their theory pointed out that a divergent contribution of thermal fluctuations in low-dimensional crystal lattices should lead to such displacements of atoms that they become comparable to interatomic distances at any finite temperature[13]. The argument was later extended by Mermin[14] and is strongly supported by an omnibus

nature materials | VOL 6 | MARCH 2007 | www.nature.com/naturematerials

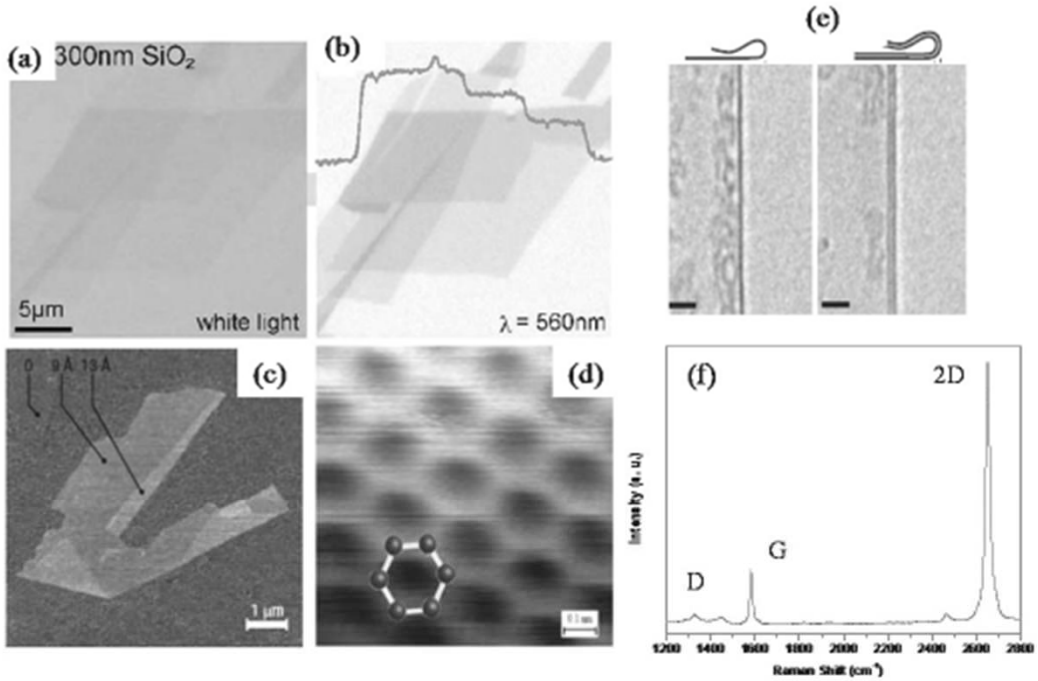

Fig. 2. Optical microscope images of graphene crystallites on 300 nm SiO_2 imaged with (a) white and (b) green light. (b) Shows step-like changes in the contrast for single, bi- and tri-layer graphenes. (c) AFM image of single-layer graphene. The folded edge exhibits a relative height of ≈4 Å indicating that it is single-layer. (d) High-resolution STM image. (e) TEM images of folded edges of single and bi-layer graphenes (From references 14, 15, 17 and 19). (f) Raman spectrum of single-layer graphene prepared by micromechanical clevage.

F. GIANNAZZO and V. RAINERI RIVISTA DEL NUOVO CIMENTO

VOL. 35, 2012 267

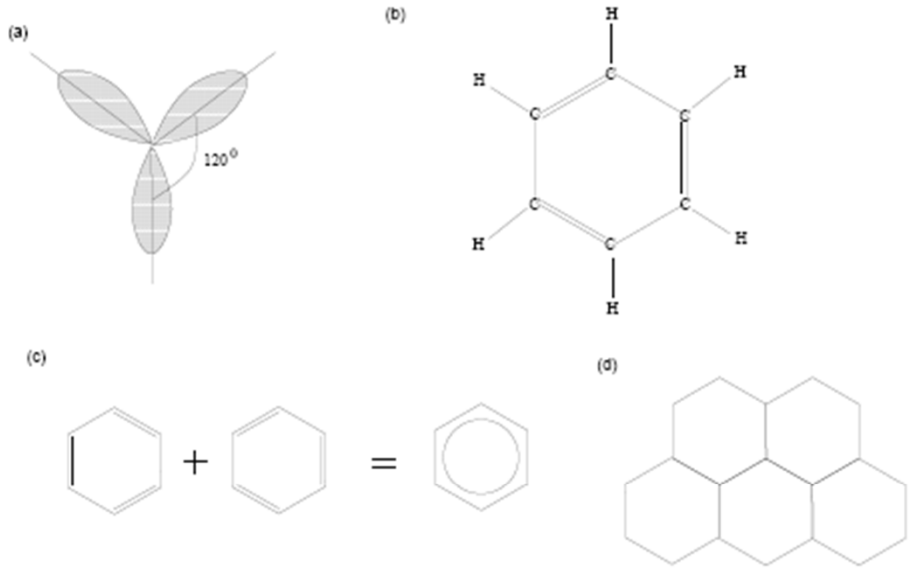

Figure 1.4: *(a)* Schematic view of the sp^2 hybridisation. The orbitals form angles of 120°. *(b)* Benzene molecule (C_6H_6). The 6 carbon atoms are situated at the corners of a hexagon and form covalent bonds with the H atoms. In addition to the 6 covalent σ bonds between the C atoms, there are three π bonds indicated by the doubled line. *(c)* The quantum-mechanical ground state of the benzene ring is a superposition of the two configurations which differ by the position of the π bonds. The π electrons are, thus, delocalised over the ring. *(d)* Graphene may be viewed as a tiling of benzene hexagons, where the H atoms are replaced by C atoms of neighbouring hexagons and where the π electrons are delocalised over the whole structure.

Il GRAFENE

Monoatomic ~0.4 nm thickness

Van-der-Waals

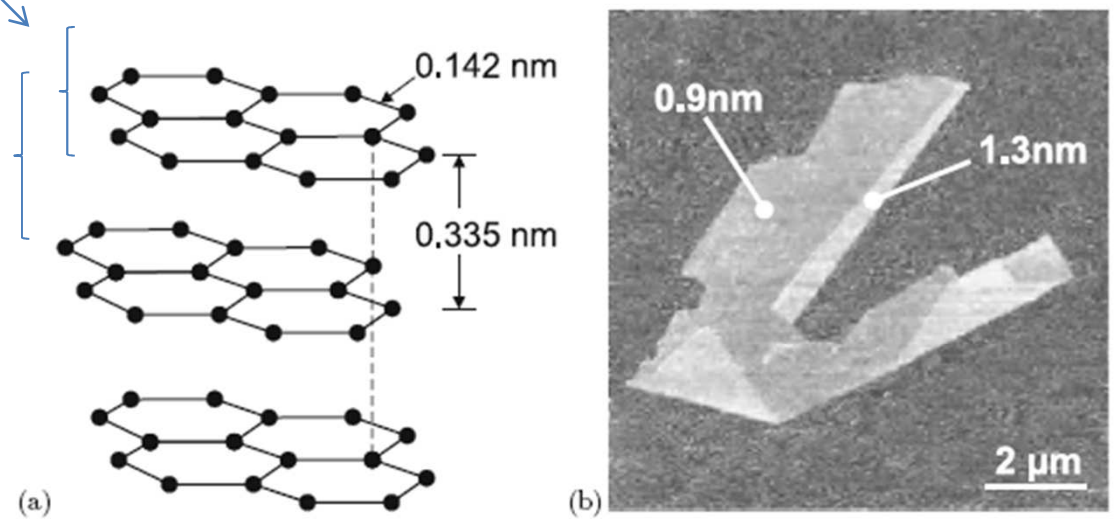

Fig. 17.2. (a) Schematic layer structure of graphite with bond length and layer distance labelled. (b) AFM image of graphene on oxidized silicon. The height of two areas relative to the background is labelled. Adapted from [1009]

Reticolo reale

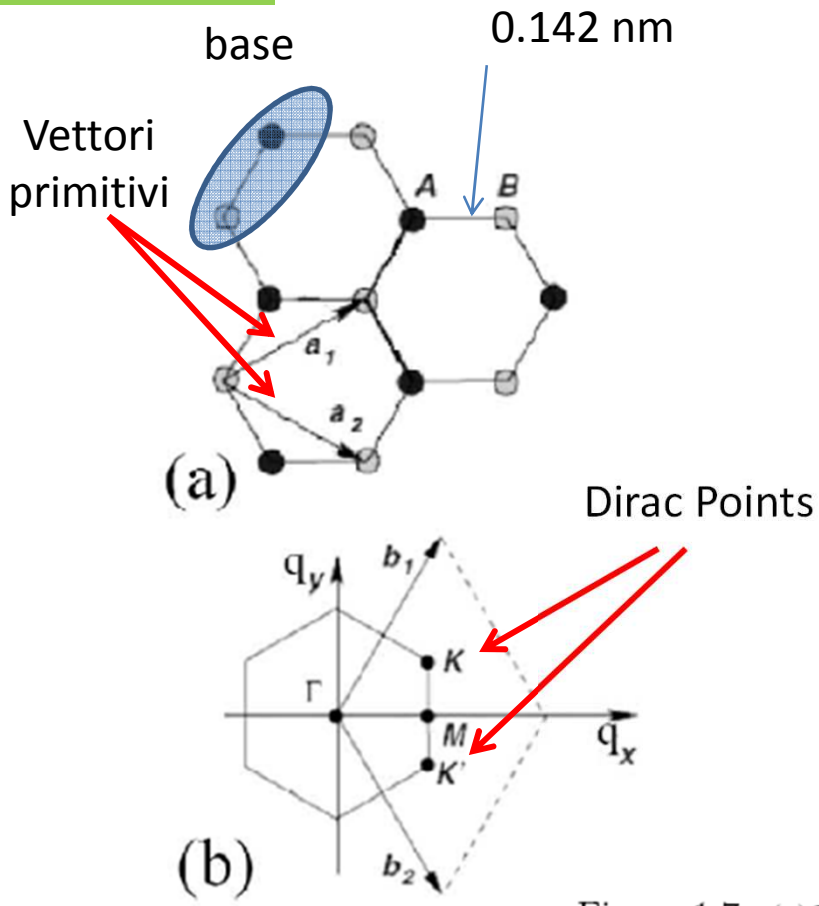

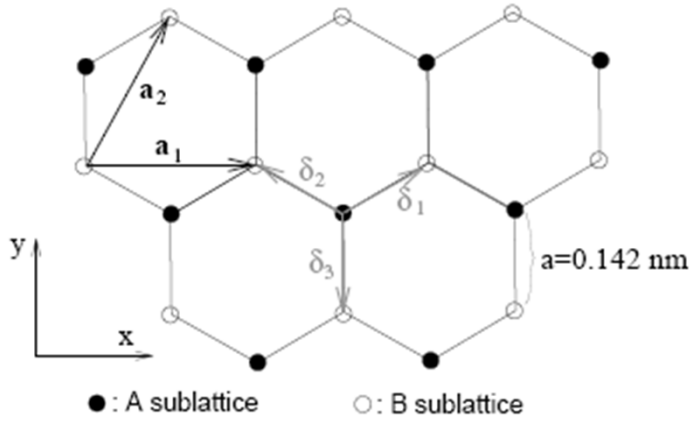

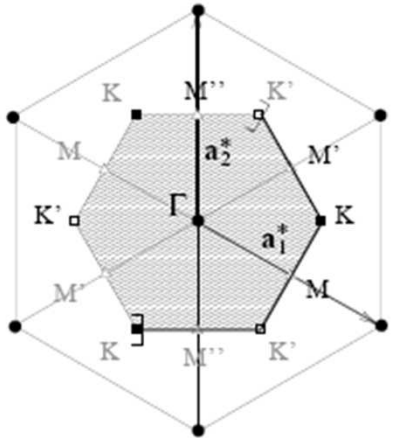

Reticolo reciproco

Figure 1.7: *(a)* Honeycomb lattice. The vectors δ_1, δ_2, and δ_3 connect *nn* carbon atoms, separated by a distance $a = 0.142$ nm. The vectors $\mathbf{a}_1$ and $\mathbf{a}_2$ are basis vectors of the triangular Bravais lattice. *(b)* Reciprocal lattice of the triangular lattice. Its primitive lattice vectors are $\mathbf{a}_1^*$ and $\mathbf{a}_2^*$. The shaded region represents the first Brillouin zone (BZ), with its centre Γ and the two inequivalent corners K (black squares) and K' (white squares). The thick part of the border of the first BZ represents those points which are counted in the definition such that no points are doubly counted. The first BZ, defined in a strict manner, is, thus, the shaded region plus the thick part of the border. For completeness, we have also shown the three inequivalent cristallographic points M, M', and M'' (white triangles).

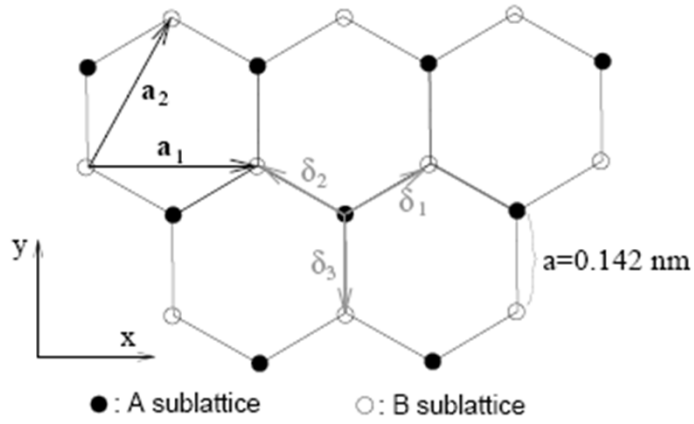

The three vectors which connect a site on the A sublattice with a *nn* on the B sublattice are given by

$$\boldsymbol{\delta}_1 = \frac{a}{2}\left(\sqrt{3}\mathbf{e}_x + \mathbf{e}_y\right), \qquad \boldsymbol{\delta}_2 = \frac{a}{2}\left(-\sqrt{3}\mathbf{e}_x + \mathbf{e}_y\right), \qquad \boldsymbol{\delta}_3 = -a\mathbf{e}_y, \quad (1.2)$$

and the triangular Bravais lattice is spanned by the basis vectors

$$\mathbf{a}_1 = \sqrt{3}a\mathbf{e}_x \qquad \text{and} \qquad \mathbf{a}_2 = \frac{\sqrt{3}a}{2}\left(\mathbf{e}_x + \sqrt{3}\mathbf{e}_y\right). \quad (1.3)$$

The modulus of the basis vectors yields the lattice spacing, $\tilde{a} = \sqrt{3}a = 0.24$ nm, and the area of the unit cell is $A_{uc} = \sqrt{3}\tilde{a}^2/2 = 0.051$ nm^2. The density of carbon atoms is, therefore, $n_C = 2/A_{uc} = 39$ nm^{-2} $= 3.9 \times 10^{15}$ cm^{-2}. Because there is one π electron per carbon atom that is not involved in a covalent σ bond, there are as many valence electrons than carbon atoms, and their density is, thus, $n_\pi = n_C = 3.9 \times 10^{15}$ cm^{-2}. As is discussed in the following chapter, this density is not equal to the carrier density in graphene, which one measures in electrical transport measurements.

Reticolo reale

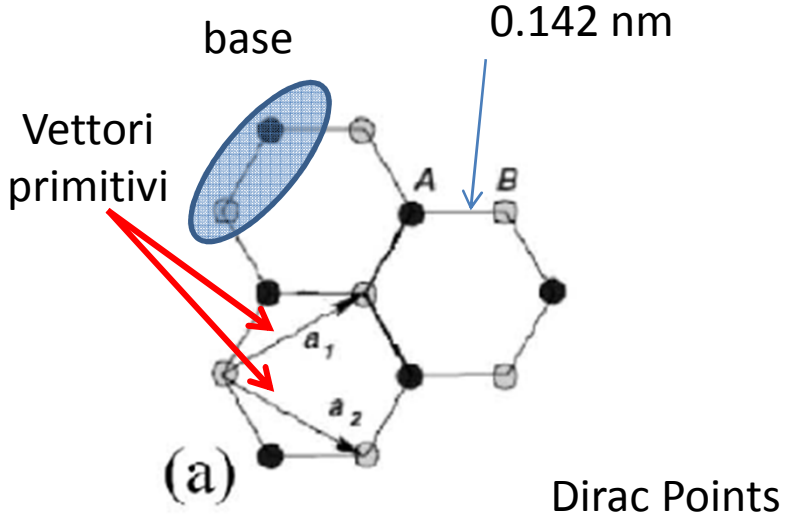

Carbonio (C) **$1s^2\ 2s^2\ 2p^2$**

Ibridizzazione sp^2

3 elettroni per atomo σ Bonds → robustezza

1 elettrone per atomo condiviso
π Bonds ⊥ alla struttura → delocalizzazione

Dirac Points

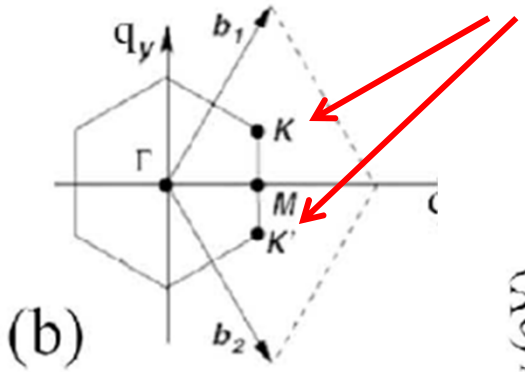

Reticolo reciproco

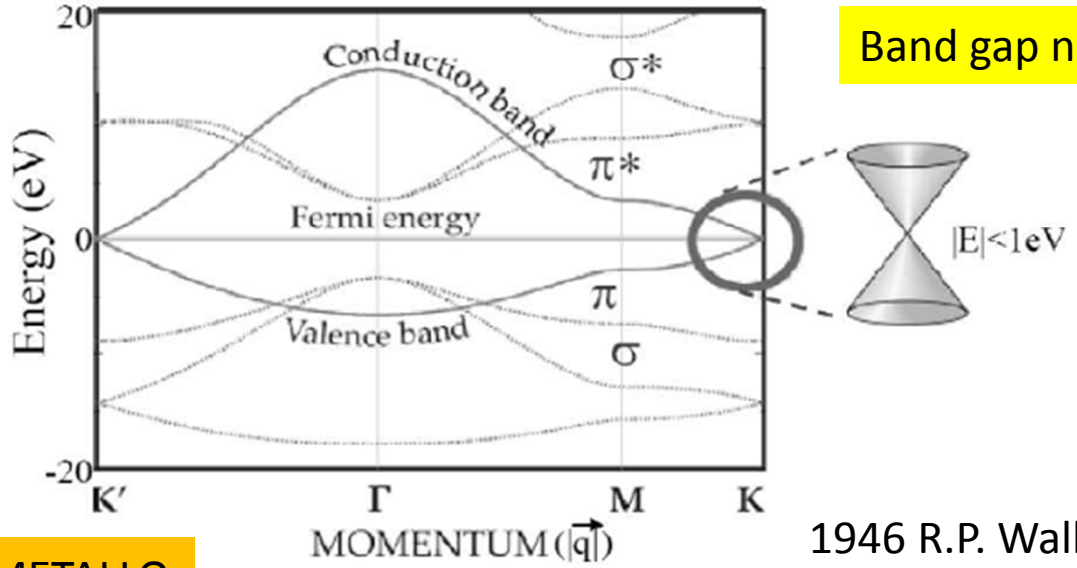

Band gap nullo

ZERO OVERLAP SEMIMETALLO

1946 R.P. Wallace

Dirac-like hamiltonian

$$\hat{H} = \hbar v_F \begin{pmatrix} 0 & k_x - ik_y \\ k_x + ik_y & 0 \end{pmatrix} = \hbar v_F \, \boldsymbol{\sigma} \cdot \mathbf{k}$$

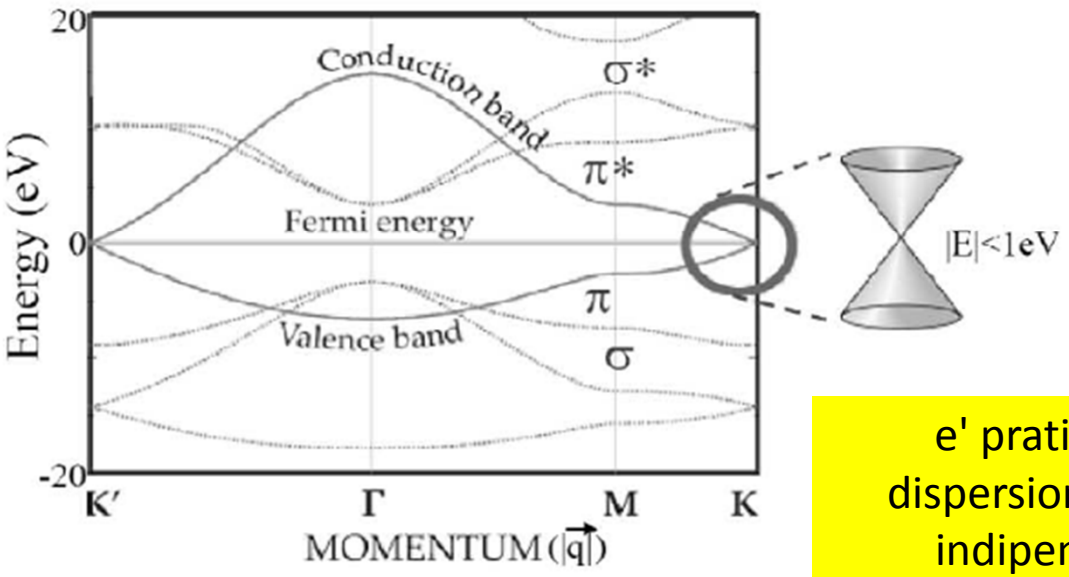

$$E_{\pm}(\vec{k}) = \pm \hbar v_F |\vec{k}\,|$$

$$v_F \simeq 1 \times 10^6 \ \mathrm{m/s},$$

e' praticamente la stessa relazione di dispersione dei fotoni che hanno velocita' indipendente dalla lunghezza d'onda

$|\vec{k}\,|$ E' misurato rispetto al punto K

Massless Dirac Fermions

Equazione di Dirac

Dirac equation *(original)*

$$\left(\beta mc^2 + c\left(\sum_{n=1}^{3} \alpha_n p_n\right)\right)\psi(x,t) = i\hbar\frac{\partial \psi(x,t)}{\partial t}$$

Elettroni relativistici nella materia

where $\psi(x,t)$ is the wave function for the electron of rest mass m with spacetime coordinates x, t. The p_1, p_2, p_3 are the components of the momentum, understood to be the momentum operator in the Schrödinger equation. Also, c is the speed of light, and $\hbar$ is the Planck constant divided by 2π. These fundamental physical constants reflect special relativity and quantum mechanics, respectively.

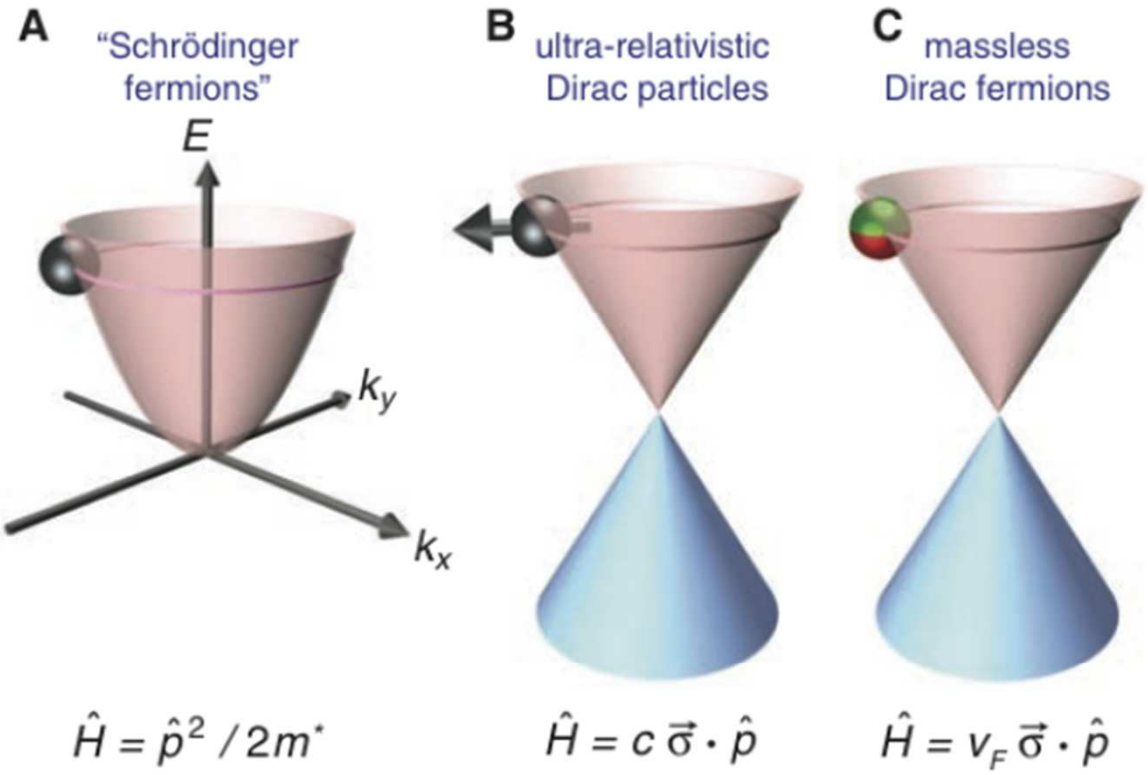

Figura 1.5 – *(A) Legge di dispersione nei normali semiconduttori per elettroni di massa efficace m^*; legge di dispersione per particelle ultrarelativistiche che si muovono alla velocità della luce (B) e alla velocità di Fermi (C).*

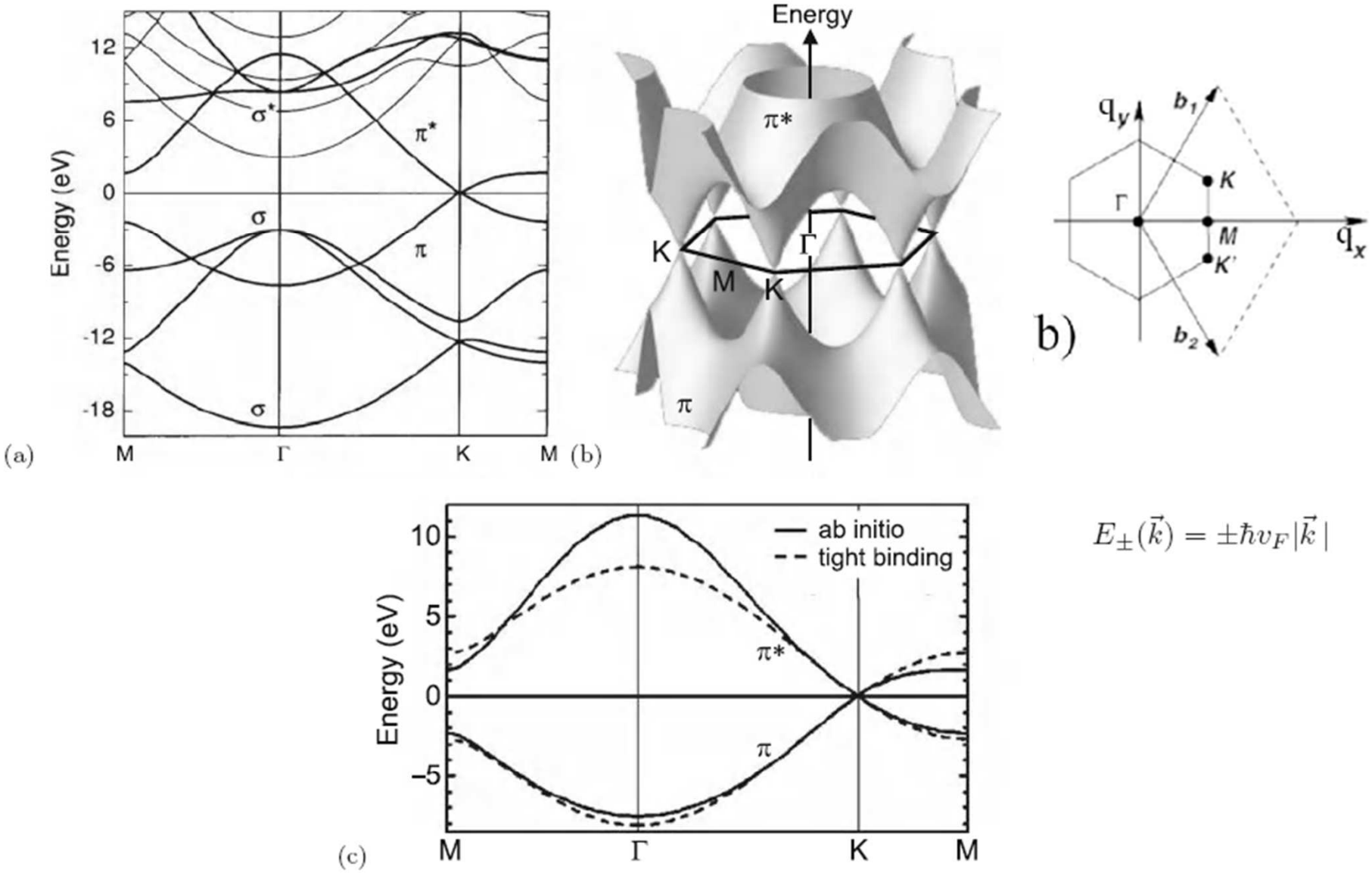

$$E_{\pm}(\vec{k}) = \pm\hbar v_F |\vec{k}\,|$$

Fig. 17.4. (**a**) Band structure of graphene from first principles. (**b**) Three-dimensional representation $E(k_x, k_y)$ of the π-bands of graphene. (**c**) Band structure of graphene with only π-bands shown, *solid* lines are ab-initio calculation, *dashed lines* are calculated with tight-binding approximation. Adapted from [1012]

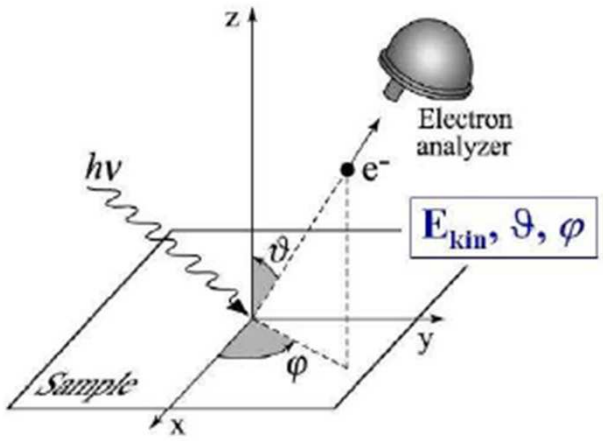

Figure 2.5: Schematic view of an ARPES measurement (from Ref. [21]) The analyser detects the energy E_f of the photoemitted electron as a function of the angles ϑ and φ, which are related to the momentum of the electronic state.

The linear dispersion relation has been experimentally measured on epitaxial graphene grown on SiC and on graphene grown on catalythic metals by angle-resolved photoemission spectroscopy (ARPES) [54]. In an ARPES map, the intensity of the photoemitted electrons is reported as a function of the energy E and of the momentum k, yielding the dispersion relation of electrons below the Fermi level.

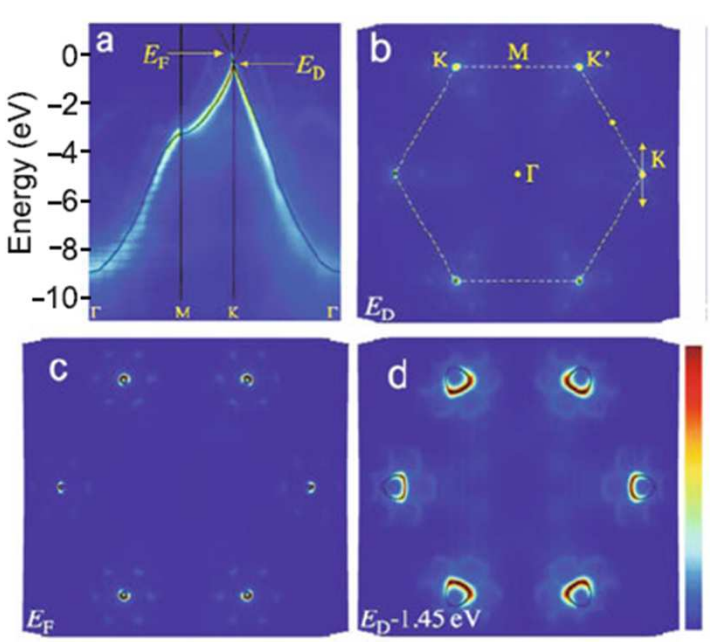

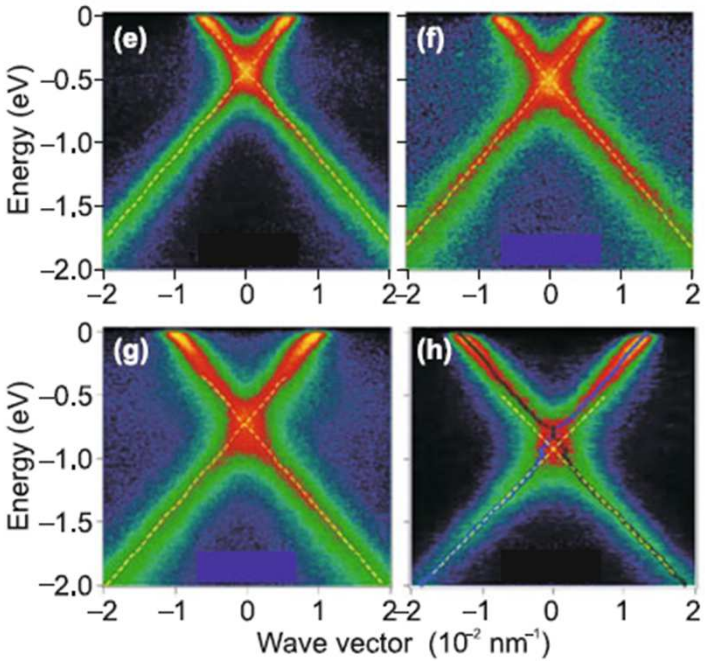

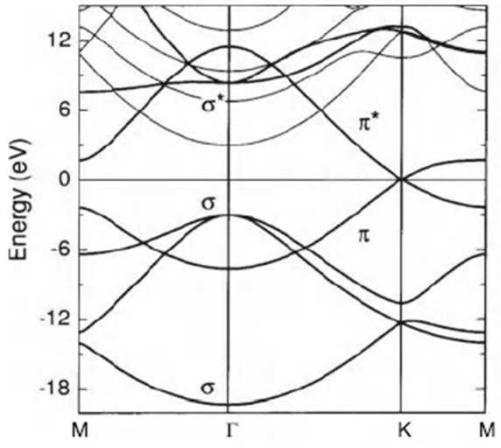

Fig. 17.5. Experimental bandstructure of graphene (on (0001) 6H-SiC) as determined from ARPES. (**a**) Energy distribution of states as a function of momentum along principal directions in the Brillouin zone. The single-orbital tight-binding model (17.2) with $T = 2.82\,\text{eV}$ is shown as *solid lines*. The Fermi level is shifted by 0.435 eV due to doping. (**b**) Constant energy map of the states at binding energy corresponding to the Dirac energy E_D; the boundary of the Brillouin Zone boundary is superimposed as *dashed line*. The arrow at the K point indicates the directions over which the data in (**e**–**h**) were acquired. (**c**, **d**) Constant energy maps at the Fermi energy ($E_\text{F} = E_\text{D} + 0.45\,\text{eV}$) and $E_\text{D} - 1.5\,\text{eV}$, respectively. (**e**–**h**) Experimental energy bands along the line through the K point parallel to Γ–M direction as indicated in (**b**). The *dashed lines* are an extrapolation of the lower bands below the Dirac crossing energy, which are observed not to pass through the upper bands (above E_D), suggesting the kinked shape of the bands around E_D. The sheet electron density is $n_\text{S} = 1.1$, 1.5, 3.7, and $5.6 \times 10^{13}\,\text{cm}^{-2}$ for (**e**)–(**h**), respectively, due to increased doping upon potassium adsorption. Adapted from [1014]

A.BOSTWICK et al. Nature Physics 2007,3, 36

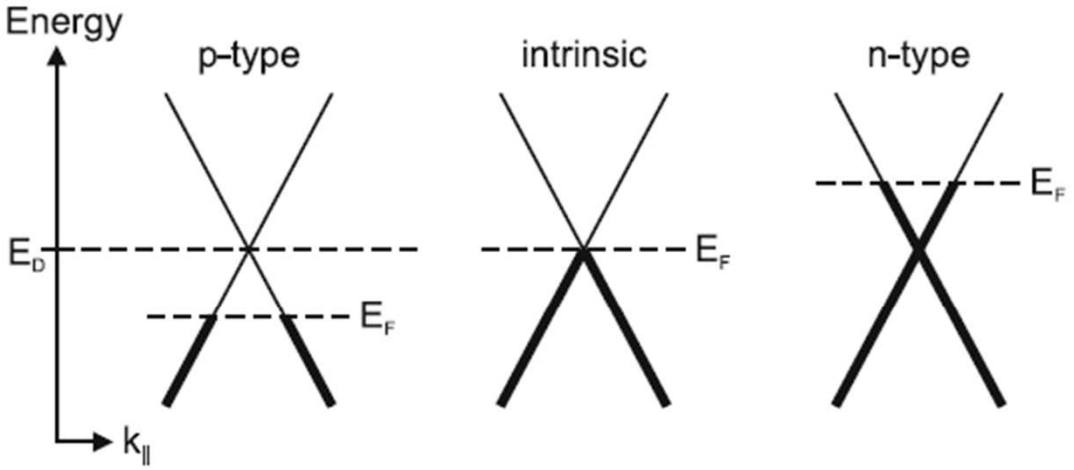

Fig. 17.7. Band structure of graphene with various positions of the Fermi energy E_F in relation to the Dirac energy E_D. States occupied with electrons are shown with in *bold*

Mobilita' poco limitata dallo scattering di fononi

Trasporto balistico bipolare

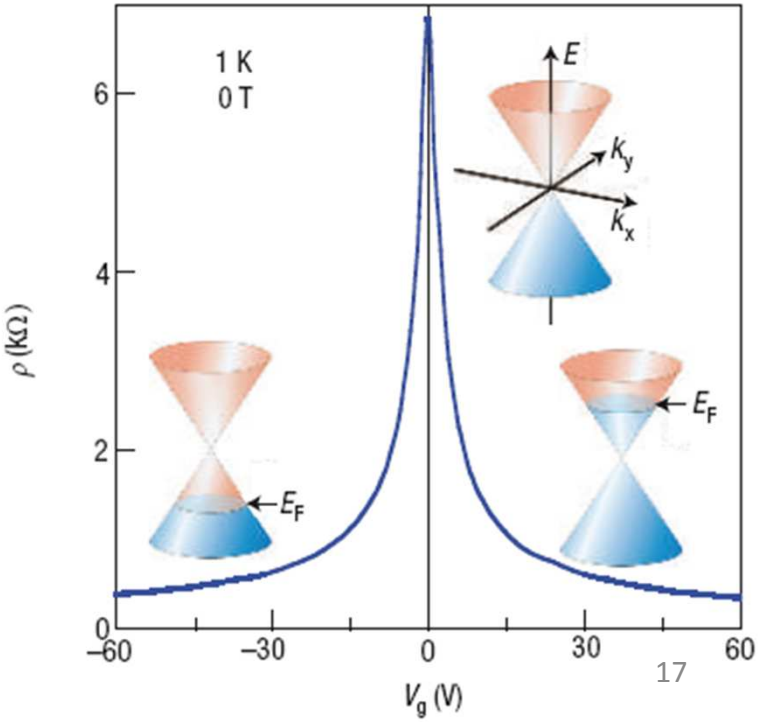

Figure 3 Ambipolar electric field effect in single-layer graphene. The insets show its conical low-energy spectrum $E(k)$, indicating changes in the position of the Fermi energy E_F with changing gate voltage V_g. Positive (negative) V_g induce electrons (holes) in concentrations $n = \alpha V_g$ where the coefficient $\alpha \approx 7.2\times10^{10}$ cm^{-2} V^{-1} for field-effect devices with a 300 nm SiO_2 layer used as a dielectric[7–9]. The rapid decrease in resistivity ρ on adding charge carriers indicates their high mobility (in this case, $\mu \approx 5{,}000$ cm^2 V^{-1} s^{-1} and does not noticeably change with increasing temperature to 300 K).

Graphene is zero band gap 2D carbon material

Molecular doping is strategically used to induce gap opening and shift of the Fermi level for electronic devices application

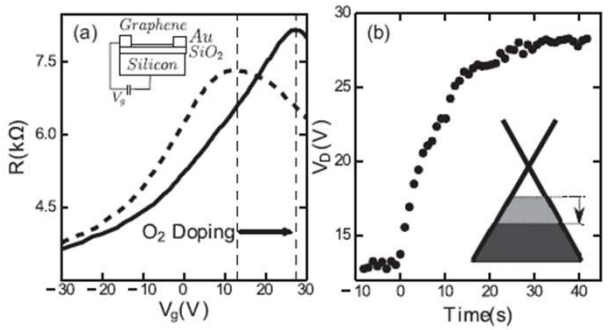

FIG. 1. (a) Resistance versus gate voltage before and after oxygen exposure (dashed and solid lines, respectively). The positions of the Dirac points are indicated by the dotted lines. The inset shows the sample layout. (b) The Dirac point position as a function of time after oxygen exposure. The oxygen was admitted to the chamber at $t = 0$ s. The inset shows the band structure of graphene with the corresponding change in the Fermi level.

S.M. Hornett et al. Phys. Rev. B 2014, 90, 081401(R)

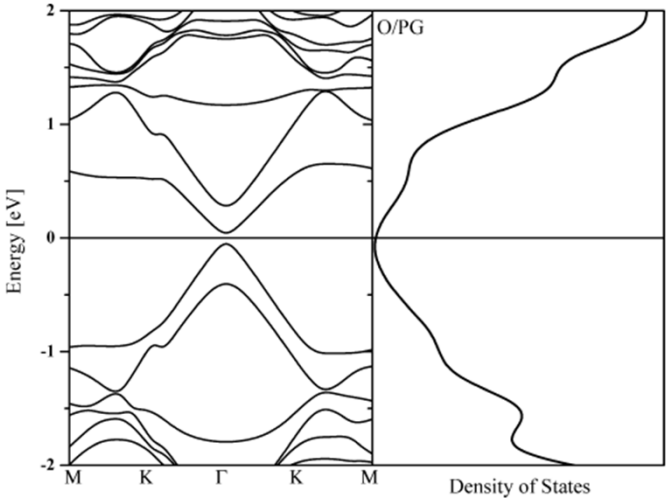

Figure 3. Band structure and total density of states of O-doped graphene.

F. Mehmood et al. J. Phys. Chem. C 2013, 117, 10366-10374

OXYGEN molecular doping

Doping of graphene to reduce sheet resistance

Modify from sp^2 hybridization to sp^3

Substitutional doping **during** Graphene growth

- p-type doping could be achieved by adding atoms with fewer valence electrons than carbon: e.g. boron (B)
- n-type doping by adding atoms with more valence electrons than carbon: e.g. nitrogen (N)

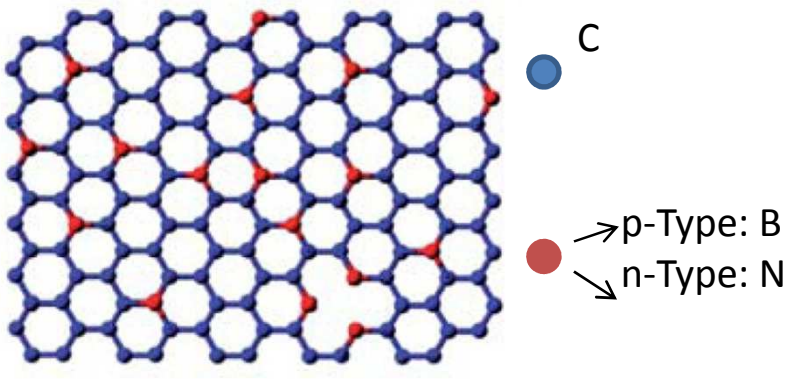

H. Liu, et al., J. Mater. Chem., 21, 2011, 3335

Post graphene growth doping by different treatments

- Surface transfer doping can be obtained by exposure of graphene to NO_2 gas for p-type doping or, for example, a ethanol gas for n-type doping.
- Photochemical oxidation in presence of UV light and oxygen.
- Thermal treatments in controlled atmosphere.

Doping vs Raman spectra

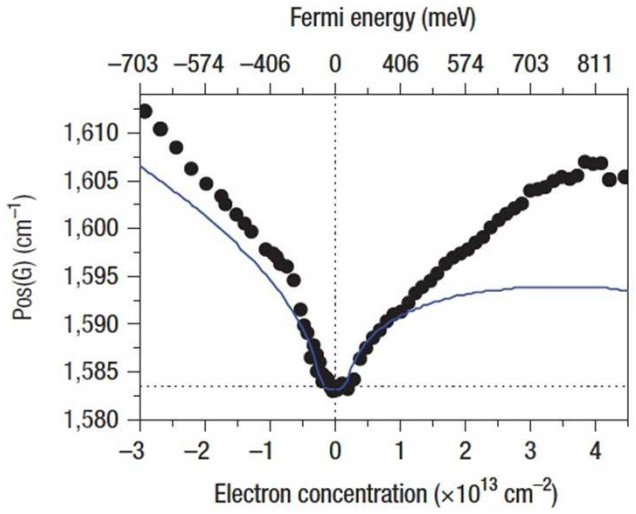

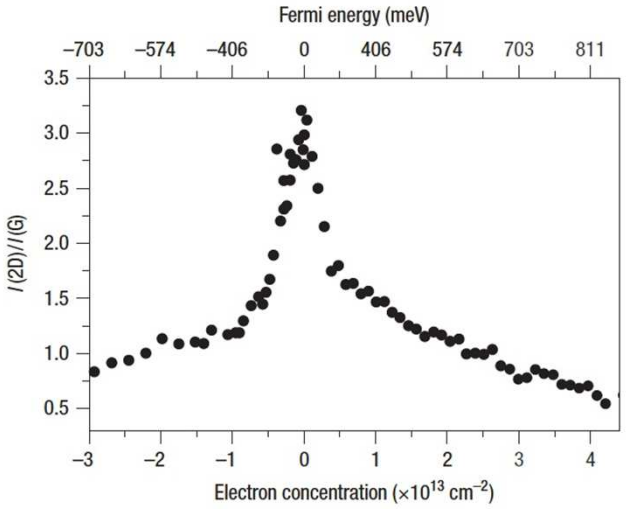

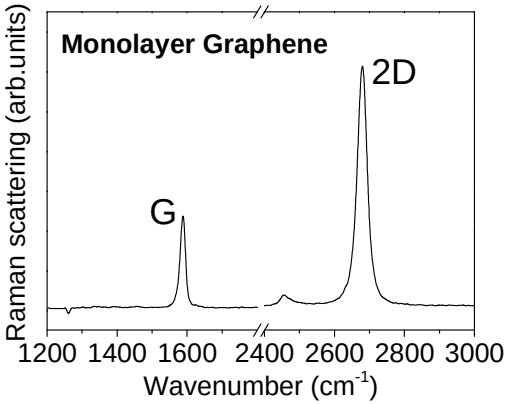

Same effects
for p-type
or n-type doping

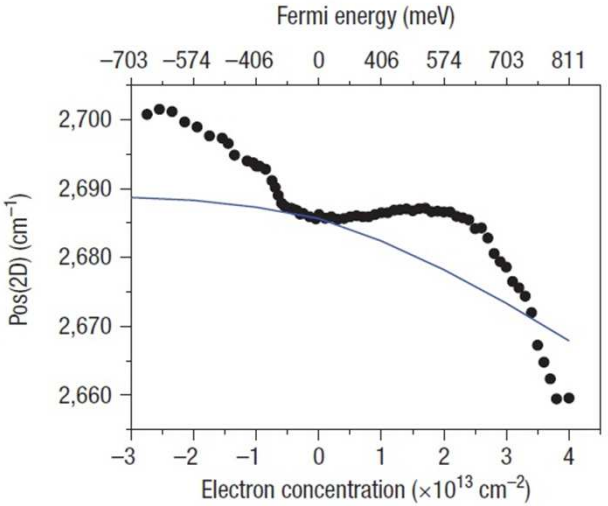

Different effects for p-type
or n-type doping

Blue shift

Red shift

A. Das et al; Nature Nanot. 2008, 3, 210

Thermally induced doping features
stability criticalities
that depend on atmosphere

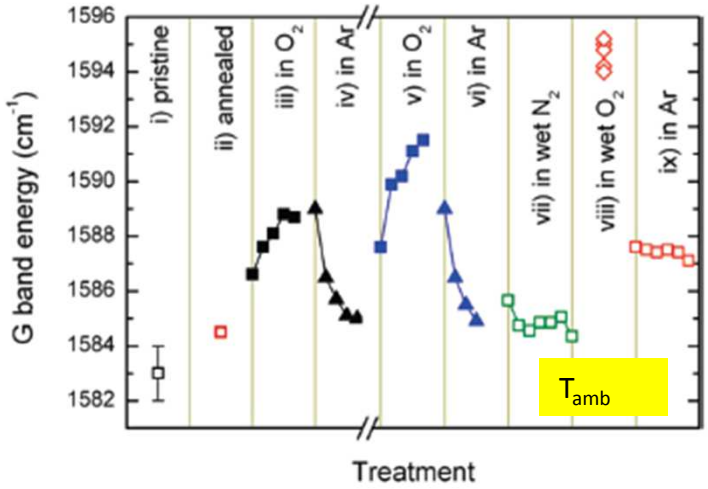

FIGURE 3. Oxygen sensitivity of 1 L graphene rippled by annealing and monitored by Raman G band energy. Raman measurements were taken at room temperature (i) in Ar atmosphere before any thermal treatment, (ii) in Ar following a two-hour annealing in Ar at 290 °C, (iii) in O_2, (iv) in Ar, (v) in O_2 following an additional two-hour annealing in Ar at 320 °C, (vi) in Ar, (vii) in N_2 containing water vapor, (viii) in O_2 containing water vapor, and (ix) in Ar. Each measurement was performed at a new spot located at least 1.5 μm away from previous spots in the graphene sample except the series of points; each series of the points in (iii) through (vii) and (ix) corresponds to consecutive measurements at one spot. Each of the five dots in (viii) was also obtained from a separate spot on the graphene. See the Supporting Information for the corresponding variations in the G band line width.

S. Ryu et al. Nano. Lett 2010, 10, 4944

TABLE II. – *Electronic properties of graphene compared with those of common bulk semiconductors and with those of the* 2DEG *at* AlGaN/GaN *heterointerface.*

	Si	Ge	GaAs	4H-SiC	GaN	AlGaN/GaN	Graphene
Energy band gap (eV)	1.1	0.67	1.47	3.3	3.4	3.4	~ 0
Electron effective mass (m^*/m_e)	1.08	0.55	0.067	0.3	0.19	0.19	~ 0
Electron mobility ($\mathrm{cm^2\,V^{-1}\,s^{-1}}$)	1350	3900	4600	800	1300	2000	2×10^5
Saturated electron drift velocity (10^7 cm/s)	1	0.6	2	2	3	3	> 5
2DEG carrier density ($\mathrm{cm^{-2}}$)						$\sim 10^{13}$	$\sim 9 \times 10^9$

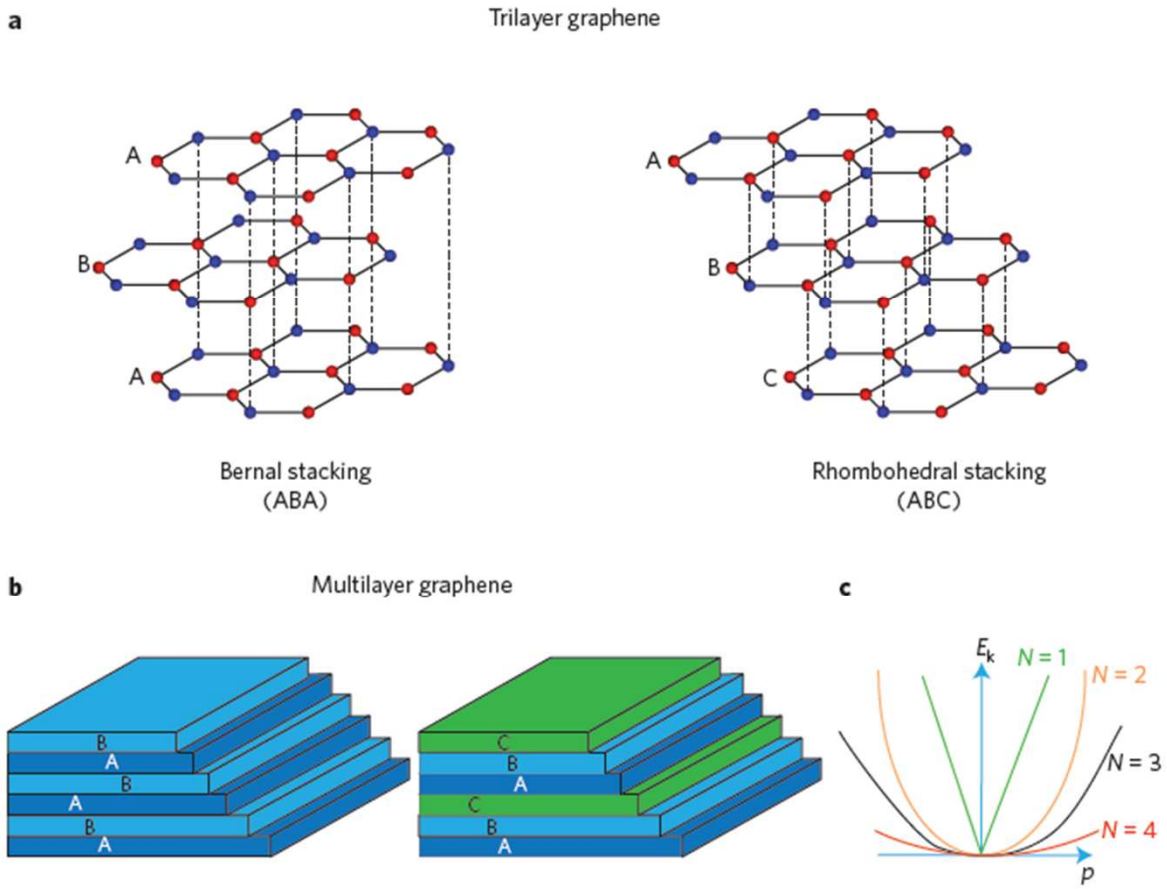

Graphene's basic structure is that of a two-dimensional hexagonal lattice with two atoms in its unit cell, denoted 'a' and 'b'. Monolayer graphene consists of a single lattice with an electronic structure that supports massless Dirac fermions with linear dispersion, $E_k \alpha p$, where E_k is the kinetic energy and p is momentum. Bilayer graphene consists of two stacked hexagonal lattices with the 'a' atom of one situated directly above the 'b' atom of the other — known as Bernal or AB stacking — and supports massive Dirac fermions with quadratic dispersion, $E_k \alpha p^2$. The intrinsic state of monolayer graphene is that of a zero-gap semimetal[5,6], whereas bilayer graphene is a semiconductor with a tunable gap[7]. But when you add a third layer, things change, and two different possibilities arise depending on how this extra layer is stacked on the others.

Zero gap

- Single layer
- Double layer
- 3<n<10 layers

Limite per considerare 2D-materials

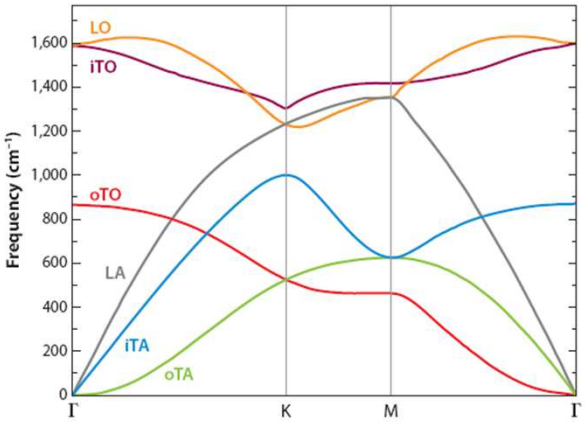

Figure 3

Calculated phonon dispersion relation of graphene showing the LO, iTO, oTO, LA, iTA, and oTA phonon branches (adapted from Reference 14).

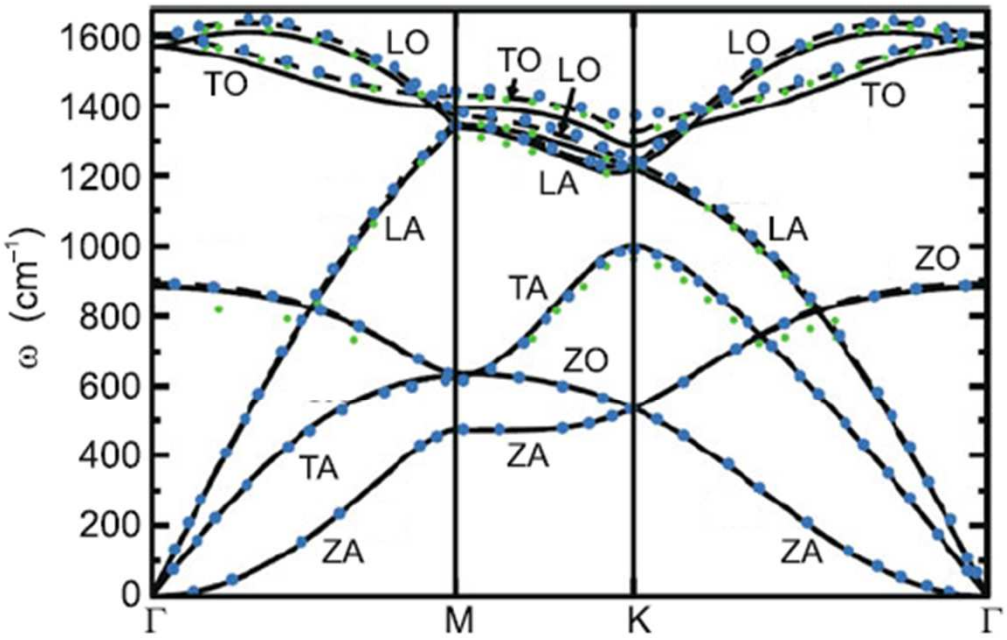

Fig. 17.3. Phonon dispersion in graphene. *Symbols* are experimental data from various methods. *Dashed lines* is DFT-LDA theory, *solid lines* GGA. Adapted from [1013]

Graphene optics

Can one expect anything interesting from the optical properties of graphene? Rather counterintuitively, despite being only one atom thick, graphene absorbs quite a large fraction of light. In the infrared limit the absorption coefficient is exactly $\pi a \approx 2.3\%$ (where $a = e^2/\hbar c$ is the fine structure constant), and the corrections to this number in the visible range of the spectrum are less than 3% [131–134]. Such a significant absorption coefficient makes it possible to see graphene without the use of a microscope; thus, one can

Another area, which should benefit significantly from the availability of CVD-grown graphene, is transparent conductive coating. Graphene is unusually optically active [131–133, 135] and for a monolayer absorbs a rather large fraction of incoming light (2.3%), but this is still significantly smaller than the typical absorption coefficient which could be achieved with a more traditional transparent conductive coating materials [155]. In conjunction with its low electrical resistivity, high chemical stability and mechanical strength, this absorption coefficient makes graphene an attractive material for optoelectronic devices.

2D Materials

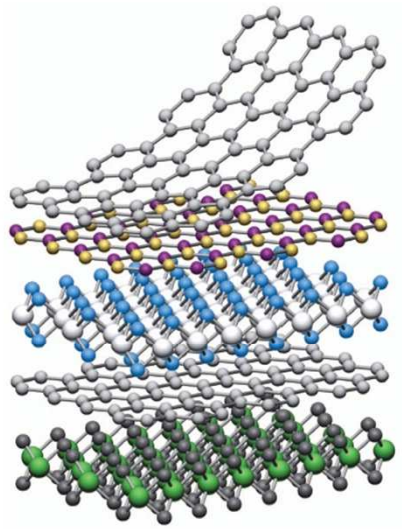

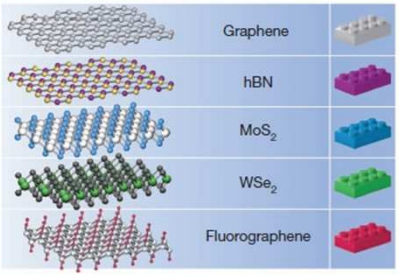

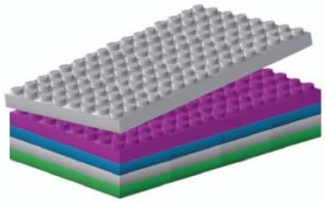

Van der Waals heterostructures

A. K. Geim[1,2] & I. V. Grigorieva[1]

Research on graphene and other two-dimensional atomic crystals is intense and is likely to remain one of the leading topics in condensed matter physics and materials science for many years. Looking beyond this field, isolated atomic planes can also be reassembled into designer heterostructures made layer by layer in a precisely chosen sequence. The first, already remarkably complex, such heterostructures (often referred to as 'van der Waals') have recently been fabricated and investigated, revealing unusual properties and new phenomena. Here we review this emerging research area and identify possible future directions. With steady improvement in fabrication techniques and using graphene's springboard, van der Waals heterostructures should develop into a large field of their own.

[1]School of Physics and Astronomy, University of Manchester, Manchester M13 9PL, UK. [2]Centre for Mesoscience and Nanotechnology, University of Manchester, Manchester M13 9PL, UK.

25 JULY 2013 | VOL 499 | NATURE | 419

Graphene family	Graphene	hBN 'white graphene'	BCN	Fluorographene	Graphene oxide
2D chalcogenides	MoS_2, WS_2, $MoSe_2$, WSe_2	Semiconducting dichalcogenides: $MoTe_2$, WTe_2, ZrS_2, $ZrSe_2$ and so on		Metallic dichalcogenides: $NbSe_2$, NbS_2, TaS_2, TiS_2, $NiSe_2$ and so on	
				Layered semiconductors: GaSe, GaTe, InSe, Bi_2Se_3 and so on	
2D oxides	Micas, BSCCO	MoO_3, WO_3	Perovskite-type: $LaNb_2O_7$, $(Ca,Sr)_2Nb_3O_{10}$, $Bi_4Ti_3O_{12}$, $Ca_2Ta_2TiO_{10}$ and so on	Hydroxides: $Ni(OH)_2$, $Eu(OH)_2$ and so on	
	Layered Cu oxides	TiO_2, MnO_2, V_2O_5, TaO_3, RuO_2 and so on		Others	

MoS_2 Transition metal dichalcogenides (TMDC)

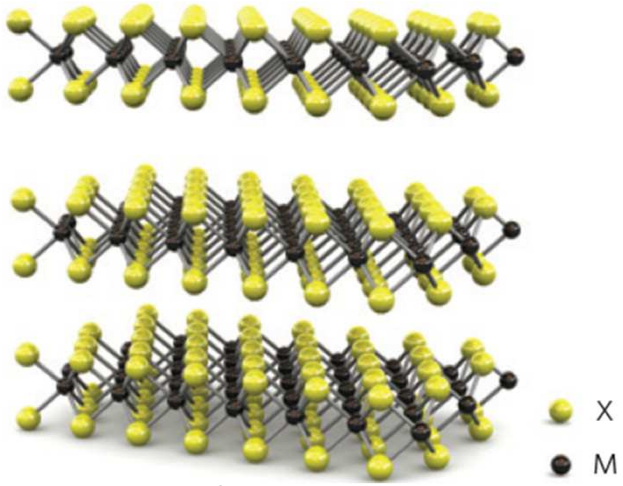

Q.H.Wang, et al, Nature Nanotechnology , 7, 2012, 193

Class of layered materials with the formula MX_2
M transition metal: Mo, W,..
X chalcogen: S, Se,...

	MoS_2	WS_2	$MoSe_2$	WSe_2
E_g(bulk), indirect	1.2 eV	1.4 eV	1.1 eV	1.2 eV
E_g(1L), direct	1.8 eV	1.9 eV	1.5 eV	1.7 eV

MoS_2 carrier mobility: 1 – 200 $cm^2V^{-1}s^{-1}$

Study of the mechanisms limiting mobility

Optical image

Morphological image (AFM)

μ-Raman Spectrum

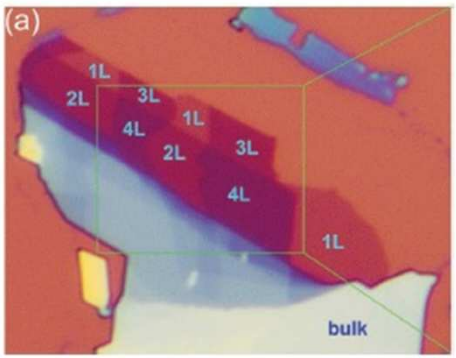

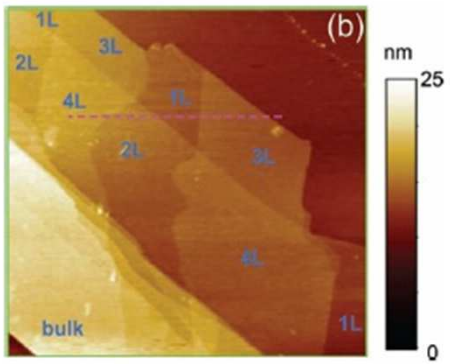

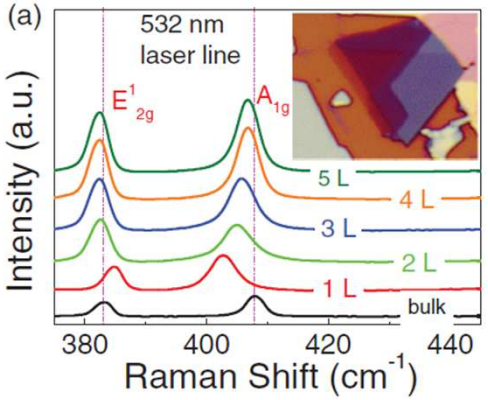

H.Li , et al, Adv. Funct. Mater. , 22, 2012, 1385.

Oxidation

PLASMA

1L

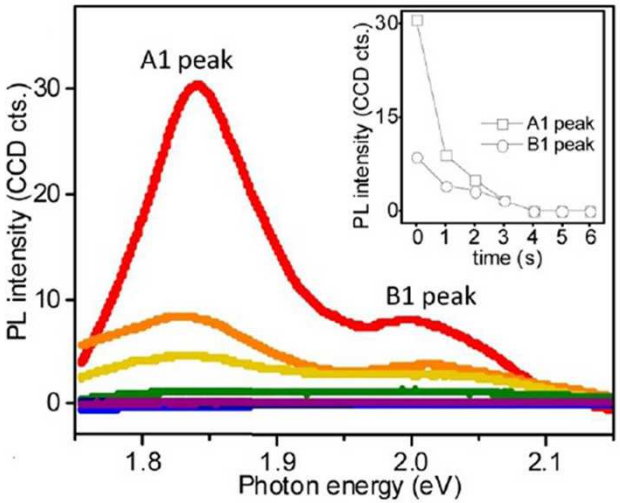

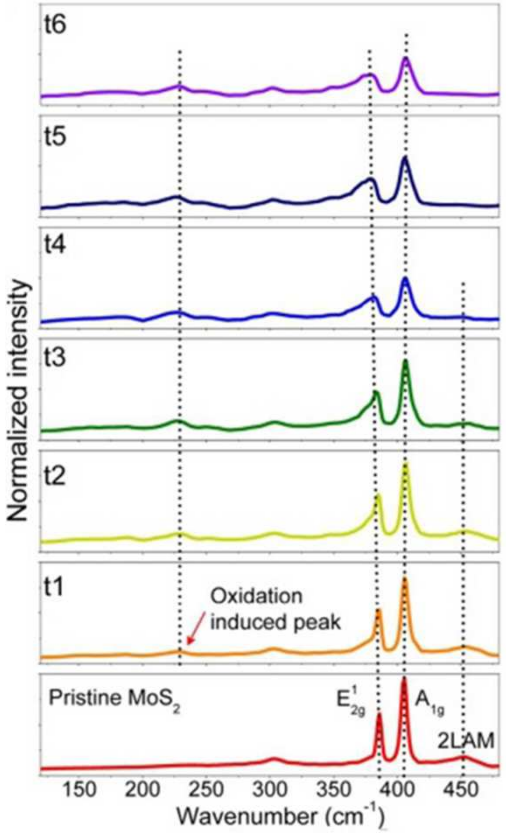

N. Kang, et al., J. Phys. Chem. C 118 (2014) 21258

THERMAL

MULTI LAYER

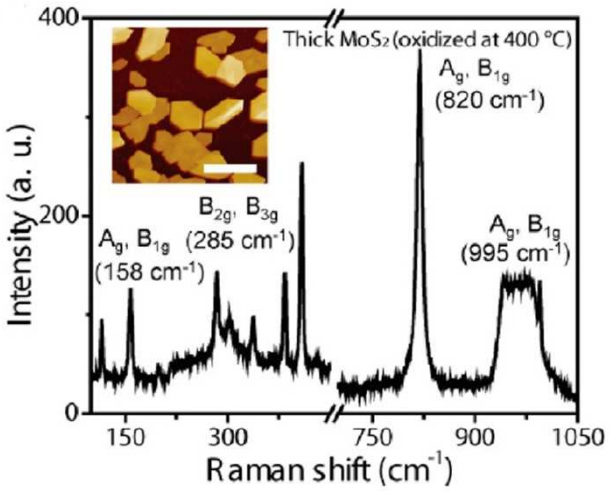

M. Yamamoto, et al., J. Phys. Chem. C 117 (2013) 25643−25649

- Proprieta' strutturali ed elettroniche
- Preparativa
- Derivati

Scotch tape method

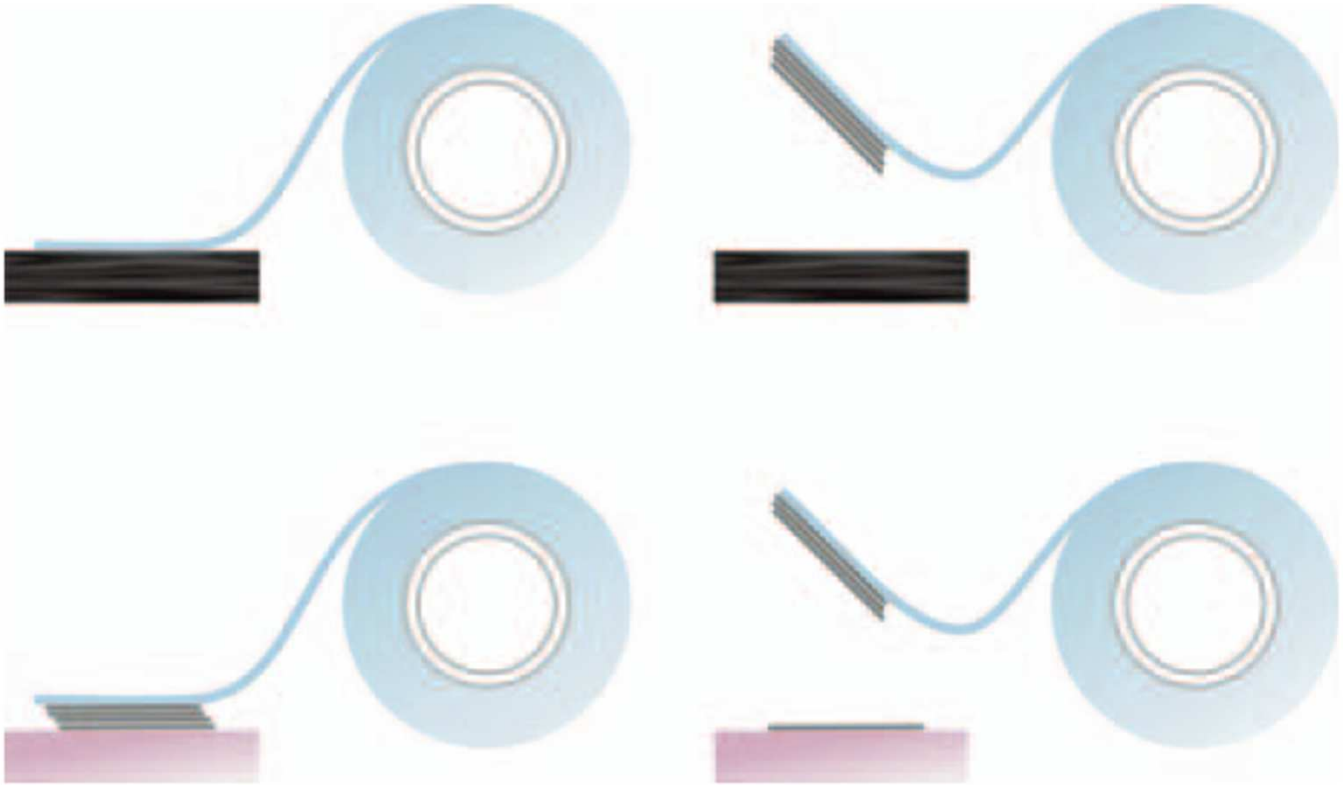

Figure 2. The micromechanical cleavage technique ('Scotch tape' method) for producing graphene. *Top row:* Adhesive tape is used to cleave the top few layers of graphite from a bulk crystal of the material. *Bottom left:* The tape with graphitic flakes is then pressed against the substrate of choice. *Bottom right:* Some flakes stay on the substrate, even on removal of the tape.

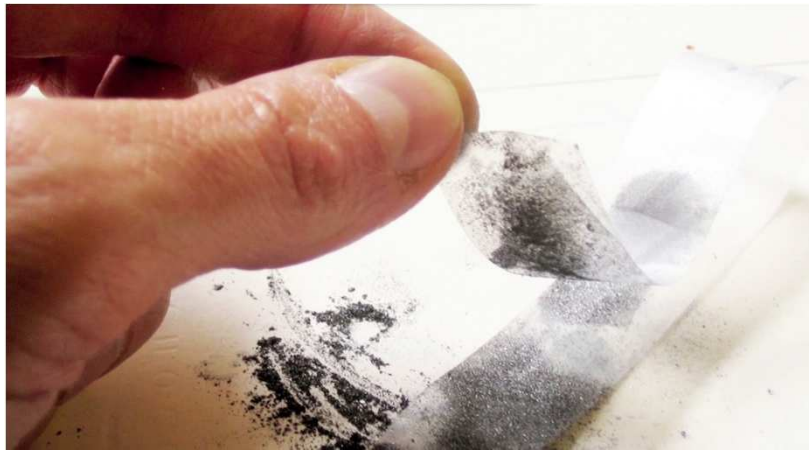

Scotch tape method

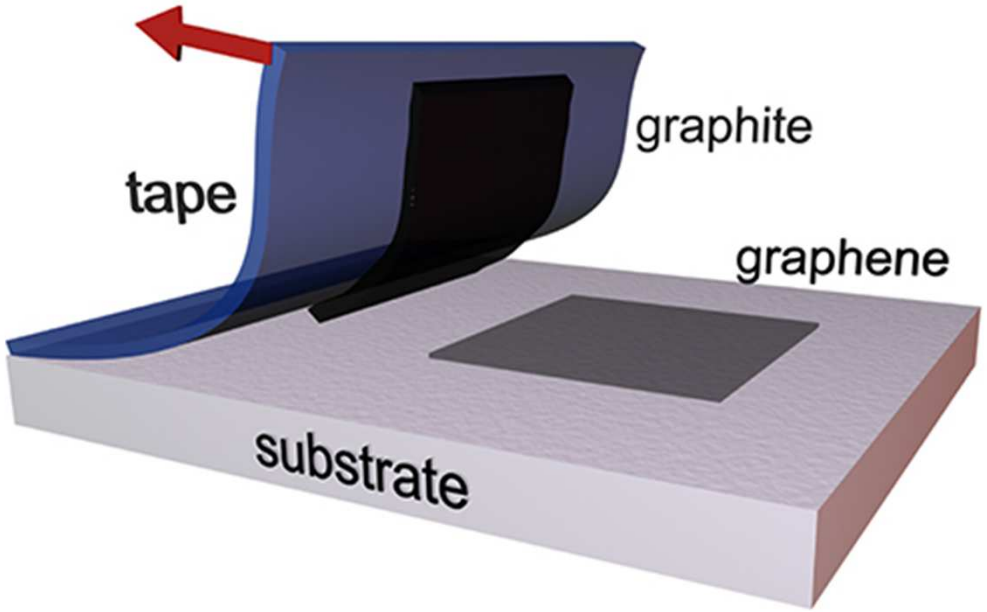

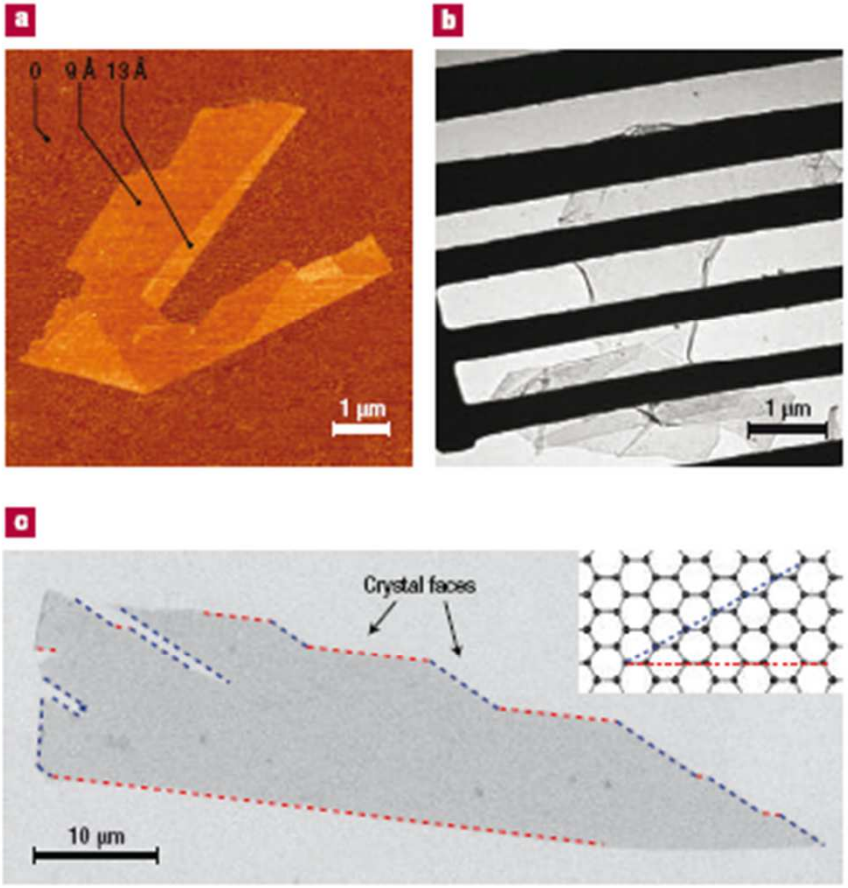

Figure 2 One-atom-thick single crystals: the thinnest material you will ever see. **a**, Graphene visualized by atomic force microscopy (adapted from ref. 8). The folded region exhibiting a relative height of ~4 Å clearly indicates that it is a single layer. (Copyright National Academy of Sciences, USA.) **b**, A graphene sheet freely suspended on a micrometre-size metallic scaffold. The transmission electron microscopy image is adapted from ref. 18. **c**, Scanning electron micrograph of a relatively large graphene crystal, which shows that most of the crystal's faces are zigzag and armchair edges as indicated by blue and red lines and illustrated in the inset (T.J. Booth, K.S.N, P. Blake and A.K.G. unpublished work). 1D transport along zigzag edges and edge-related magnetism are expected to attract significant attention.

The critical ingredient for success was the observation that graphene becomes visible in an optical microscope if placed on top of a Si wafer with a carefully chosen thickness of SiO_2, owing to a feeble interference-like contrast with respect to an empty wafer. If not for this simple yet effective way to scan substrates in search of graphene crystallites, they would probably remain undiscovered today. Indeed, even knowing the exact recipe[8], it requires special care and perseverance to find graphene. For example, only a 5% difference in SiO_2 thickness (315 nm instead of the current standard of 300 nm) can make single-layer graphene completely invisible. Careful selection of the initial graphite material (so that it has largest possible grains) and the use of freshly cleaved and cleaned surfaces of graphite and SiO_2 can also make all the difference. Note that graphene was recently[37,38] found to have a clear signature in Raman microscopy, which makes this technique useful for quick inspection of thickness, even though potential crystallites still have to be first hunted for in an optical microscope.

GROWING GRAPHENE FILMS

Researchers make large (centimetre-scale) graphene films by depositing carbon atoms from a vapour onto a copper surface. Roll-to-roll processing then transfers the graphene film from copper to another substrate.

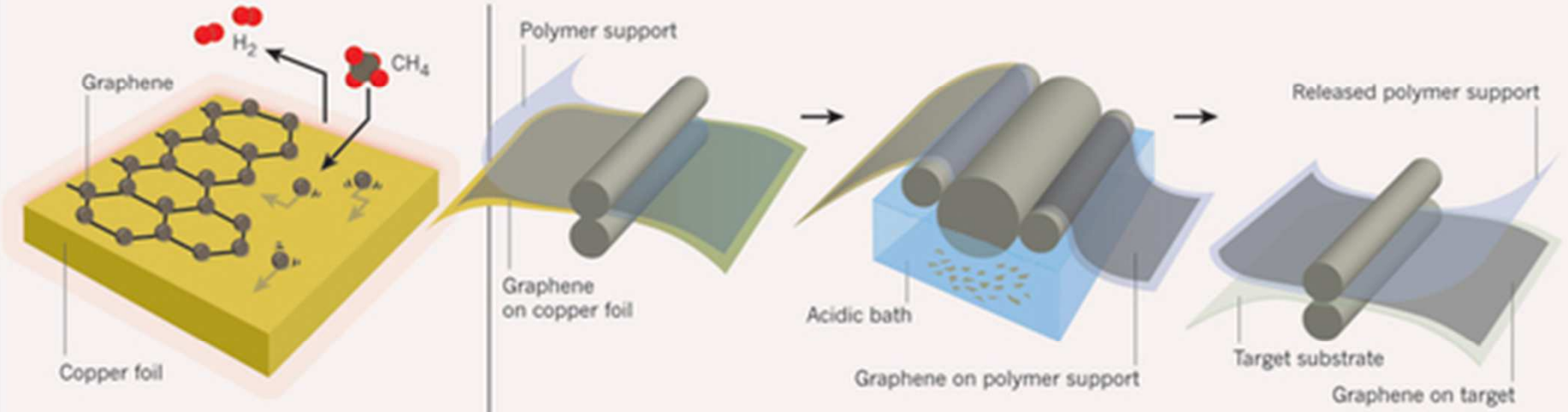

Copper foil is heated to 800-1000°C in a furnace, where hydrogen (H_2) and methane gas (CH_4) are piped through. Carbon atoms grow as graphene film on top of the copper.

Adhesive 'thermal release' tape is attached on top of the graphene, by applying pressure between heavy rollers.

The copper is eaten away in a plastic bath filled with etchant (such as ammonium persulfate, a bleaching agent and oxidant).

On heating to 90-120°C, the adhesive tape unsticks, leaving the graphene clinging to a target substrate.

CVD Graphene + transfer

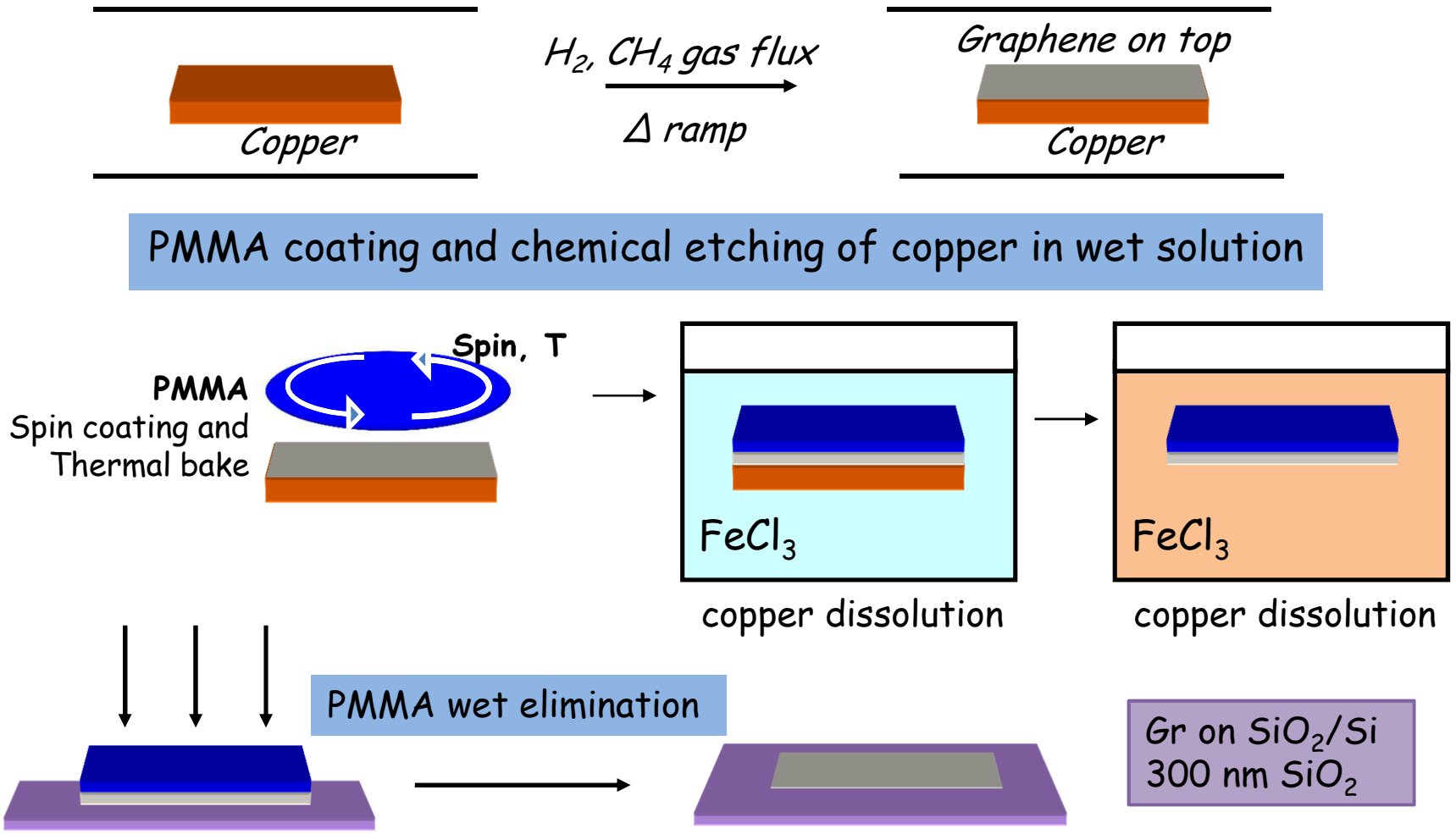

- Proprieta' strutturali ed elettroniche
- Preparativa
- Derivati

2D Materials

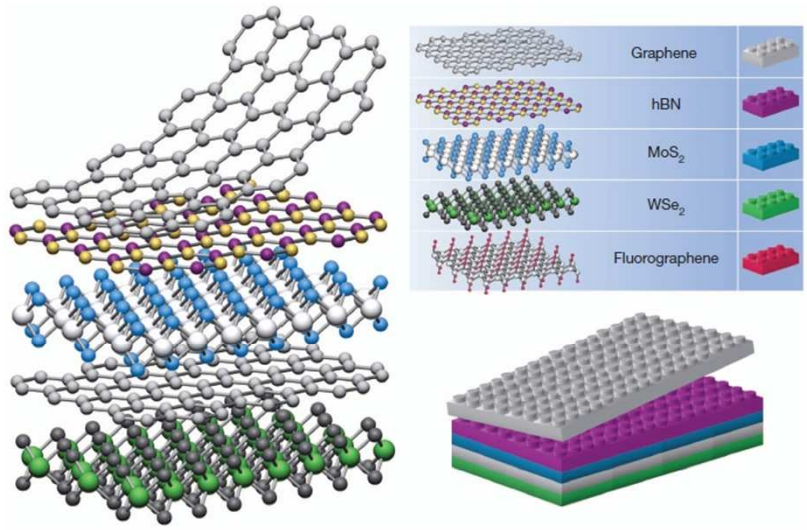

Van der Waals heterostructures

A. K. Geim[1,2] & I. V. Grigorieva[1]

Research on graphene and other two-dimensional atomic crystals is intense and is likely to remain one of the leading topics in condensed matter physics and materials science for many years. Looking beyond this field, isolated atomic planes can also be reassembled into designer heterostructures made layer by layer in a precisely chosen sequence. The first, already remarkably complex, such heterostructures (often referred to as 'van der Waals') have recently been fabricated and investigated, revealing unusual properties and new phenomena. Here we review this emerging research area and identify possible future directions. With steady improvement in fabrication techniques and using graphene's springboard, van der Waals heterostructures should develop into a large field of their own.

[1]School of Physics and Astronomy, University of Manchester, Manchester M13 9PL, UK. [2]Centre for Mesoscience and Nanotechnology, University of Manchester, Manchester M13 9PL, UK.

25 JULY 2013 | VOL 499 | NATURE | 419

Graphene family	Graphene	hBN 'white graphene'	BCN	Fluorographene	Graphene oxide
2D chalcogenides	MoS_2, WS_2, $MoSe_2$, WSe_2	Semiconducting dichalcogenides: $MoTe_2$, WTe_2, ZrS_2, $ZrSe_2$ and so on		Metallic dichalcogenides: $NbSe_2$, NbS_2, TaS_2, TiS_2, $NiSe_2$ and so on	
				Layered semiconductors: GaSe, GaTe, InSe, Bi_2Se_3 and so on	
2D oxides	Micas, BSCCO	MoO_3, WO_3	Perovskite-type: $LaNb_2O_7$, $(Ca,Sr)_2Nb_3O_{10}$, $Bi_4Ti_3O_{12}$, $Ca_2Ta_2TiO_{10}$ and so on	Hydroxides: $Ni(OH)_2$, $Eu(OH)_2$ and so on	
	Layered Cu oxides	TiO_2, MnO_2, V_2O_5, TaO_3, RuO_2 and so on		Others	

Graphene oxide

Interest in Graphene Oxide

Graphene Oxide

Graphene precursor

Total Reduction
- Chemical
- Thermal
- Irradiation

Partial Reduction
- Photoluminescence
- Tunable resistivity
- Solubility

Surface Functionalization

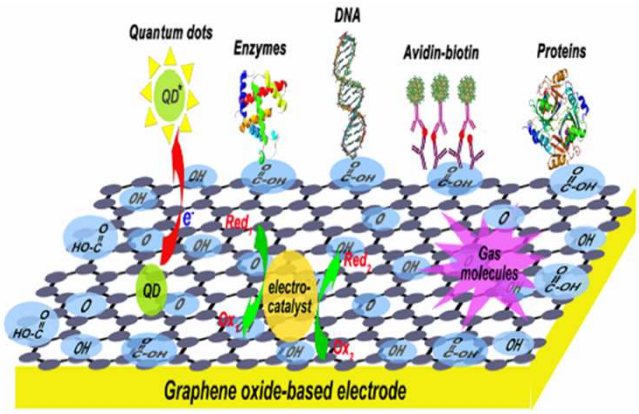

D. Chen et al.

dx.doi.org/10.1021/cr300115g | *Chem. Rev.* 2012, 112, 6027–6053

Specific surface
~2600 m^2/g

Preparation

GrO from graphite flakes by MARCANO modified Hummers method

D.C. Marcano et al. *ACS NANO* (2010) 4, 4806

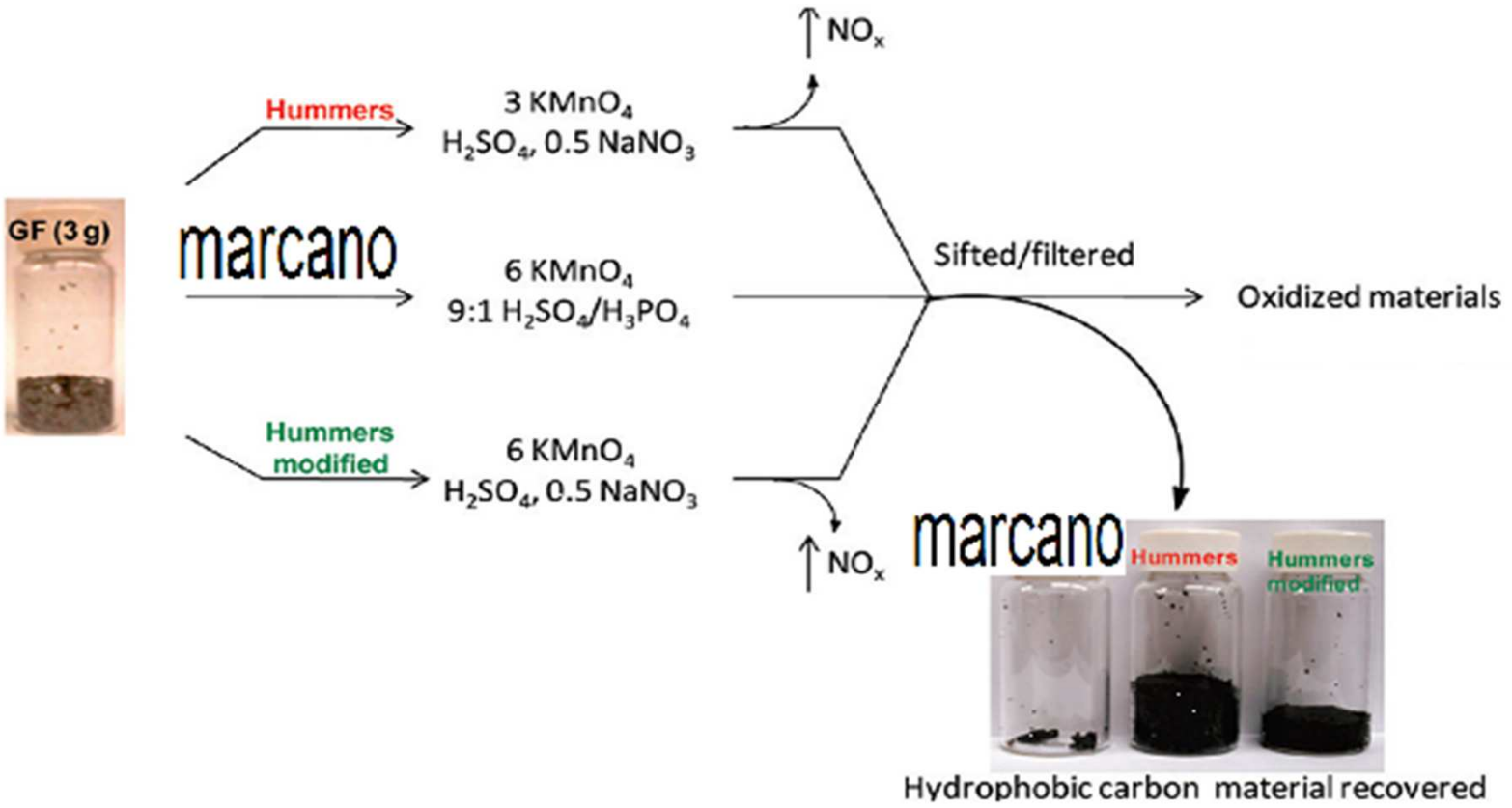

STRUCTURE

Graphene Oxide as an Ideal Substrate for Hydrogen Storage

VOL. 3 ▪ NO. 10 ▪ 2995–3000 ▪ 2009 ACSNANO

Lu Wang,[†,‡] Kyuho Lee,[‡] Yi-Yang Sun,[‡] Michael Lucking,[‡] Zhongfang Chen,[§] Ji Jun Zhao,[†] and Shengbai B. Zhang[‡,*]

[†]Laboratory of Materials Modification by Laser, Electron, and Ion Beams, School of Physics and Optoelectronic Technology and College of Advanced Science and Technology, Dalian University of Technology, Dalian 116024, China, [‡]Department of Physics, Applied Physics, and Astronomy, Rensselaer Polytechnic Institute, Troy, New York 12180, and [§]Department of Chemistry, Institute for Functional Nanomaterials, University of Puerto Rico, San Juan, Puerto Rico 00931

RESULTS AND DISCUSSION

Structural Models. As mentioned before, GO structural model from experiment is not available. Recently, Cai and co-workers investigated the structure of GO by solid-state NMR experiments.[25] They found that −O− and −OH are the two dominant O groups on the surface by clearly distinguishing three types of C atoms, namely, the sp^2 carbon and two types of sp^3 carbon bonded to hydroxyls and epoxies, respectively. The concentrations of these three types of carbon are comparable, suggesting that the C(sp^2)/C(−O−)/C(−OH) ratio of 1:1:1 is representative of the GO. Moreover, it suggests that the two types of O groups are in proximity, possibly as nearest neighbors.

EPOXY

HYDROXYL

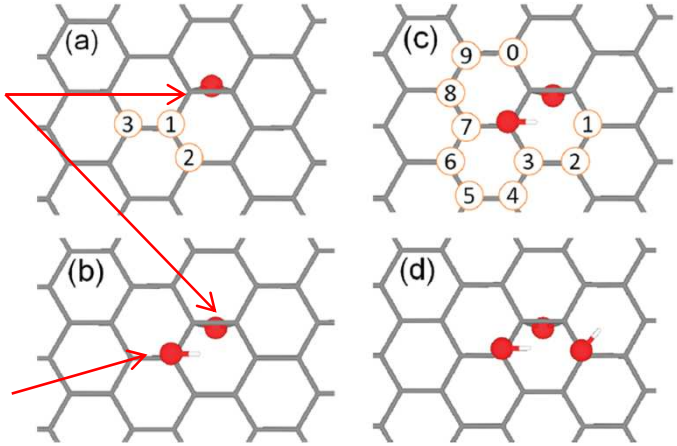

Figure 1. (a) Possible positions to form an (−O−, −OH) pair, (b) the most stable (−O−, −OH) pair, (c) possible positions to form an (−O−, 2−OH) complex starting from (b), and (d) one of the most stable (−O−, 2−OH) motifs, which is used throughout the paper.

STRUCTURE

Graphene Oxide as an Ideal Substrate for Hydrogen Storage

VOL. 3 ▪ NO. 10 ▪ 2995–3000 ▪ 2009 ACSNANO

Lu Wang,[†,‡] Kyuho Lee,[‡] Yi-Yang Sun,[‡] Michael Lucking,[‡] Zhongfang Chen,[§] Ji Jun Zhao,[†] and Shengbai B. Zhang[‡,*]

[†]Laboratory of Materials Modification by Laser, Electron, and Ion Beams, School of Physics and Optoelectronic Technology and College of Advanced Science and Technology, Dalian University of Technology, Dalian 116024, China, [‡]Department of Physics, Applied Physics, and Astronomy, Rensselaer Polytechnic Institute, Troy, New York 12180, and [§]Department of Chemistry, Institute for Functional Nanomaterials, University of Puerto Rico, San Juan, Puerto Rico 00931

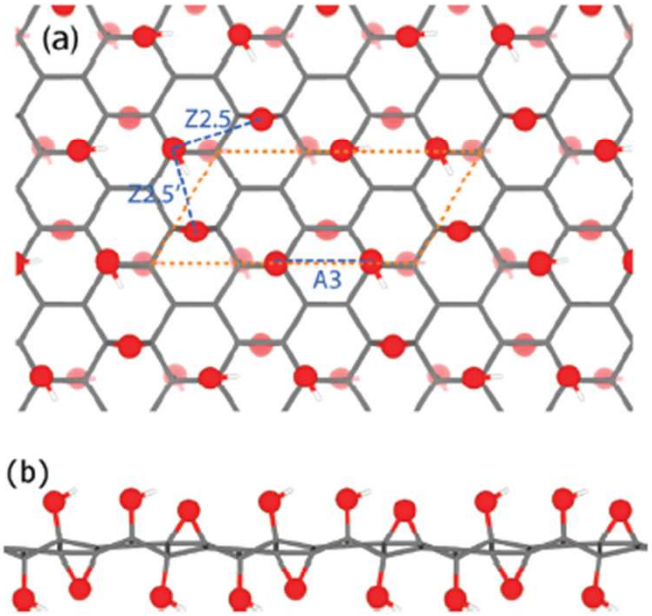

Figure 2. GO model constructed by spatially repeating the motif in Figure 1d. (a) Top view. (b) Side view (along the armchair direction). Dashed lines define the $2\sqrt{3} \times \sqrt{3}$ supercell. Note that all the −OH form H bonds with neighboring −OH or −O−, and both −O− groups are distributed evenly on both sides of the graphene sheet. The Ti sites are *Z*2.5, *Z*2.5′, or *A*3, where *Z* stands for *zig-zag* and *A* stands for *armchair*, and the number indicates the separation between O atoms (in units of C−C bonds along the carbon chain). Due to the high O packing density, each Ti always binds to two O.

PHOTOLUMINESCENCE

Materials Views
www.MaterialsViews.com

ADVANCED MATERIALS
www.advmat.de

COMMUNICATIO

DOI: 10.1002/adma.200901996

Adv. Mater. **2010**, *22*, 505–509

Blue Photoluminescence from Chemically Derived Graphene Oxide

By *Goki Eda, Yun-Yue Lin, Cecilia Mattevi, Hisato Yamaguchi, Hsin-An Chen, I-Sheng Chen, Chun-Wei Chen,* and Manish Chhowalla**

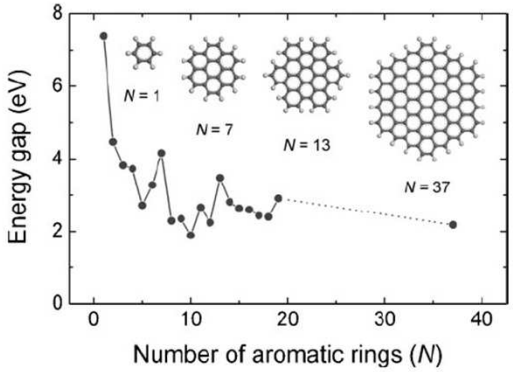

Figure 2. Energy gap of π–π* transitions calculated based on DFT as a function of the number of fused aromatic rings (*N*). The inset shows the structures of the graphene molecules used for calculation.

responsible for the blue emission observed here. Figure 2 shows that the calculated gap between the highest occupied molecular orbital (HOMO) and the lowest unoccupied molecular orbital (LUMO) of a single benzene ring is ~7 eV, which decreases down to ~2 eV for a cluster of 20 aromatic rings. Thus, we expect that much smaller sp^2 clusters of few aromatic rings or of some other sp^2 configuration of similar size are likely to be responsible for the observed blue PL. Our previously proposed structural model for GO takes into account both the larger sp^2 domains and also the smaller sp^2 fragments that are responsible for the transport of carriers between the larger sp^2 domains.[14] In this view, the observed increase in the PL intensity without energy shift during the initial reduction treatments may be attributed to the increased concentration of such sp^2 fragments. Furthermore, the subsequent PL quenching with longer reduction may be the result of percolation among these sp^2 configurations, facilitating transport of excitons to nonradiative recombination sites.

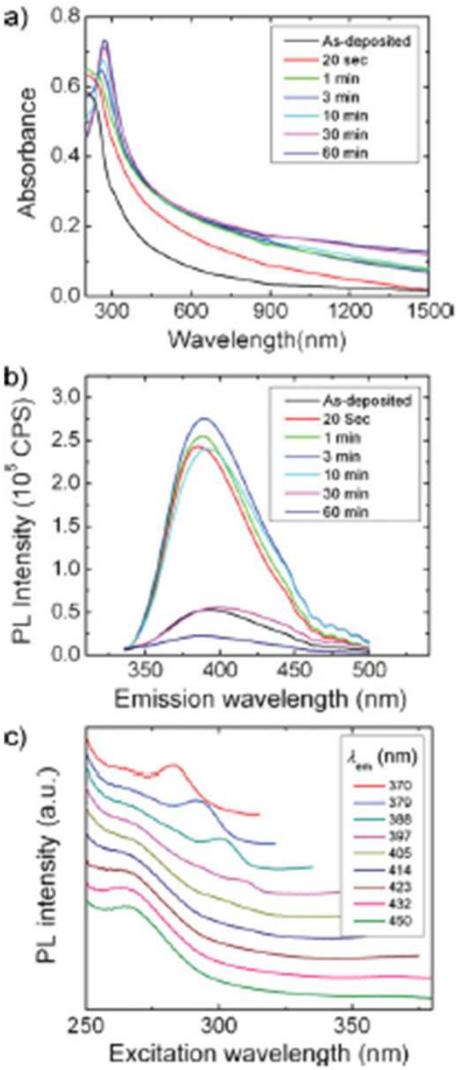

Figure 1. a) Absorbance and b,c) photoluminescence spectra of progressively reduced GO thin films. The total time of exposure to hydrazine is noted in the legend. The photoluminescence spectra in (b) were obtained for excitation at 325 nm. The PL excitation spectra in (c) were obtained for different wavelengths of the emission spectrum ranging from 370 to 450 nm.

MODEL

Materials Views
www.MaterialsViews.com

ADVANCED MATERIALS
www.advmat.de

Blue Photoluminescence from Chemically Derived Graphene Oxide

By Goki Eda, Yun-Yue Lin, Cecilia Mattevi, Hisato Yamaguchi, Hsin-An Chen, I-Sheng Chen, Chun-Wei Chen,* and Manish Chhowalla*

COMMUNICATIO

DOI: 10.1002/adma.200901996

Adv. Mater. 2010, 22, 505–509

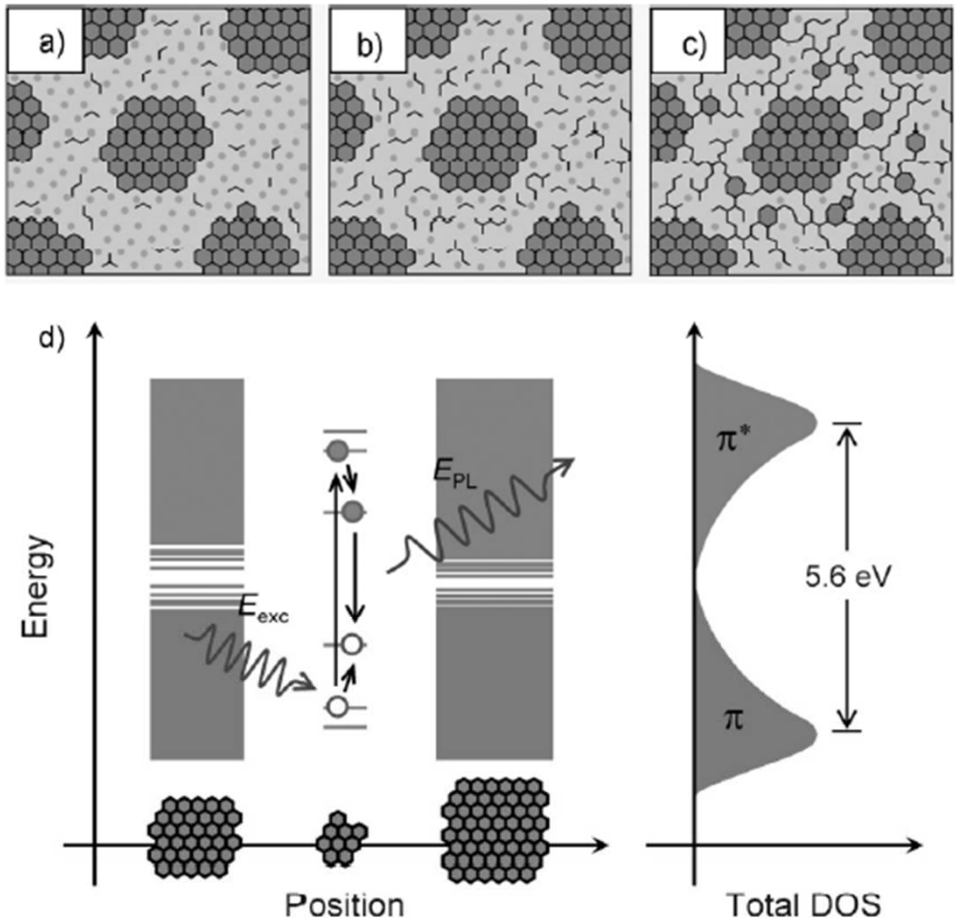

Figure 4. a–c) Structural models of GO at different stages of reduction. The larger sp^2 clusters of aromatic rings are not drawn to scale. The smaller sp^2 domains indicated by zigzag lines do not necessarily correspond to any specific structure (such as olefinic chains for example) but to small and localized sp^2 configurations that act as the luminescence centers. The PL intensity is relatively weak for (a) as-synthesized GO but increases with reduction due to (b) formation of additional small sp^2 domains between the larger clusters because of evolution of oxygen with reduction. After extensive reduction, the smaller sp^2 domains create (c) percolating pathways among the larger clusters. d) Representative band structure of GO. The energy levels are quantized with large energy gap for small fragments due to confinement. A photogenerated e–h pair recombining radiatively is depicted.

NANOPARTICLES COMPOSITE

Graphene/TiO_2 nano-composite for photocatalytic removal of pharmaceuticals from water

Zahra Gholamvand [1], Anne Morrissey [2], Kieran Nolan [3], John Tobin[4]
1,4 School of Biotechnology, 3 School of Chemical Sciences ,2 Oscail, Dublin City University, Dublin 9, Ireland
Email: Zahra.gholamvand2@mail.dcu.ie

Nano-crystalline semiconductors, such as Titania, are important in energy-saving processes including: water purification, air purification, disinfection and self-cleaning.

Principle

When titanium dioxide (TiO_2) absorbs UV light, electron and holes are produced. The positive hole breaks apart the water molecule to form hydrogen gas and hydroxyl radical. The negative-electron reacts with oxygen to form super oxide anion. These species can break down a wide variety of organic materials, organic acids, estrogens, pesticides, dyes, crude oil, microbes.

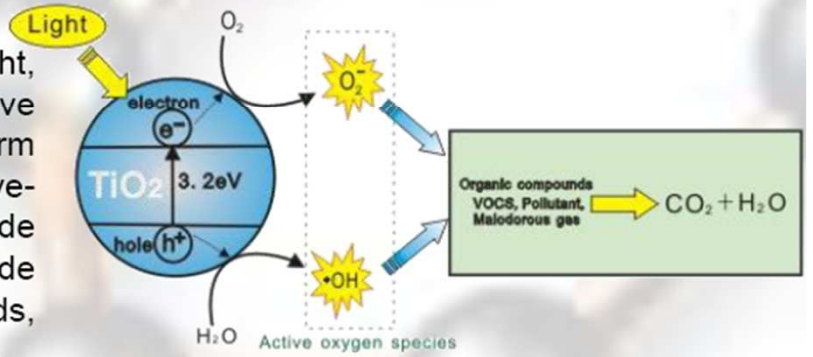

Incorporating $TiO_2$with an adsorbent .Graphene was chosen because it has high transparency, high conductivity, high surface area and many functional group for TiO_2 binding

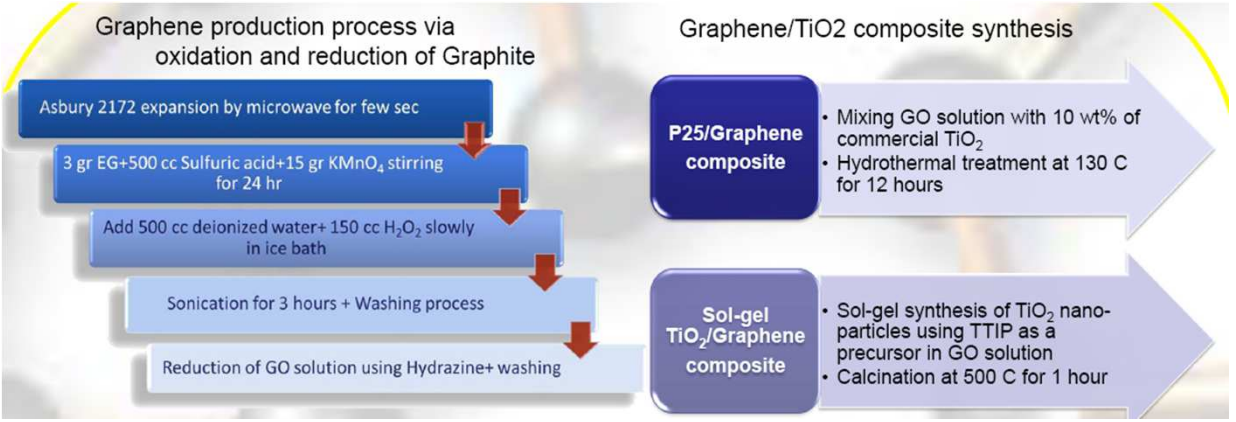

CHEMICAL REVIEWS
Review
pubs.acs.org/CR
dx.doi.org/10.1021/cr300115g | *Chem. Rev.* 2012, 112, 6027–6053

GrO FUNCTIONALIZATION

Graphene Oxide: Preparation, Functionalization, and Electrochemical Applications

Da Chen,[†,‡] Hongbin Feng,[†] and Jinghong Li*[,†]

[†]Department of Chemistry, Tsinghua University, Beijing 100084, China
[‡]College of Materials Science & Engineering, China Jiliang University, Hangzhou 310018, China

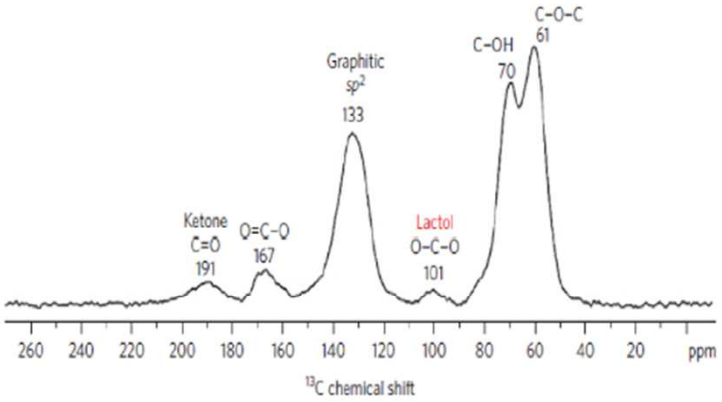

(A)

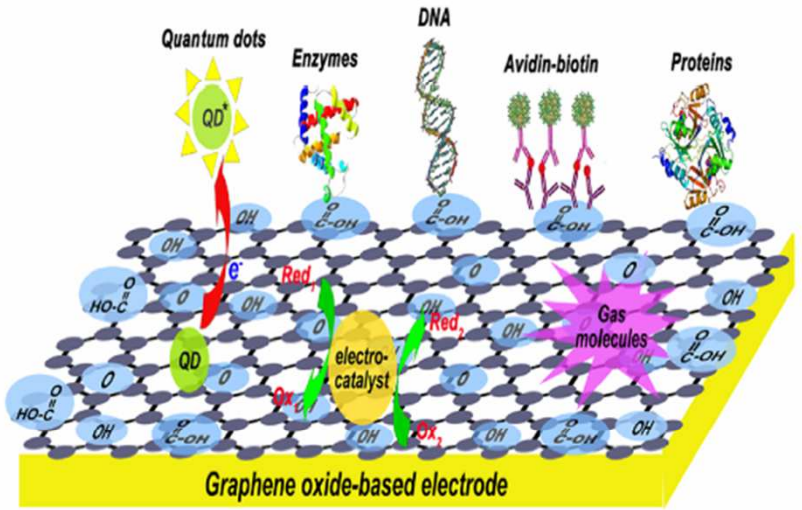

Figure 1. Schematic illustration of GO-based electrodes for electrochemical applications.

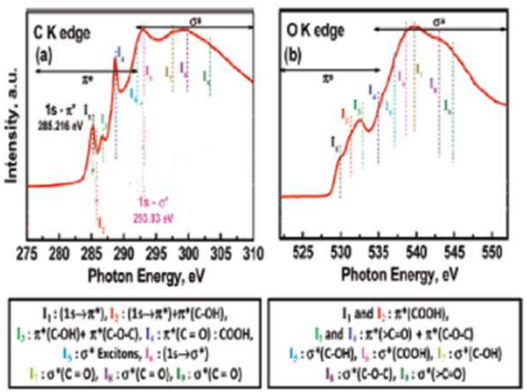

(B)

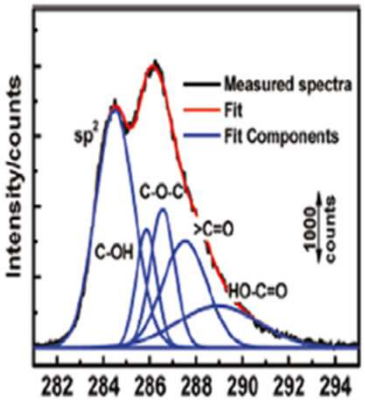

(C)

Figure 4. (A) Solid-state ^{13}C magic-angle spinning (MAS) NMR spectra of GO. Reprinted with permission from ref 40. Copyright 2009 Nature Publishing Group. (B) High-resolution (a) C K-edge and (b) O K-edge synchrotron XANES spectra of GO. Reprinted with permission from ref 81. Copyright 2011 American Chemical Society. (C) High-resolution C1s XPS spectra of GO. Reprinted with permission from ref 81. Copyright 2011

GrO-SiO_2 composites

Langmuir Article pubs.acs.org/Langmuir dx.doi.org/10.1021/la3009283 | Langmuir 2012, 28, 7055−7062

Silica-Graphene Oxide Hybrid Composite Particles and Their Electroresponsive Characteristics

Wen Ling Zhang and Hyoung Jin Choi*

As a new potential application of GO, both GO/conducting polyaniline nanocomposite[13] and GO coated core−shell structured polystyrene microspheres[14] were recently reported to show electroresponsive electrorheological (ER) characteristics under an applied electric field. Note that the ER fluids are in general heterogeneous dispersions composed of micrometer-sized polarizable particles dispersed in low-dielectricity oils, such as silicone oil or mineral oil.[15,16] They are considered smart/intelligent materials since their structural and rheological characteristics can change reversibly under external electric fields.[17,18] The particles become polarized and behave as Bingham fluids. Since their discovery, these smart materials have a range of applications in the scientific and engineering communities, particularly in the areas of electromechanical devices including shock absorbers, engine mounts, and clutches because of their rapid response to an electrical field and their controllable mechanical properties.[19] Extrinsically polarizable particles, such as semiconducting polymers, as well as their derivatives,[20−22] high dielectric inorganics including silica and porous silica/polymer nanocomposites, clay/polymer nanocomposites, and TiO_2 nanoparticles have been reported extensively as important ER materials.[23−26]

Scheme 1. Schematic Diagram of Synthesis Process of Si-GO Hybrid Composite

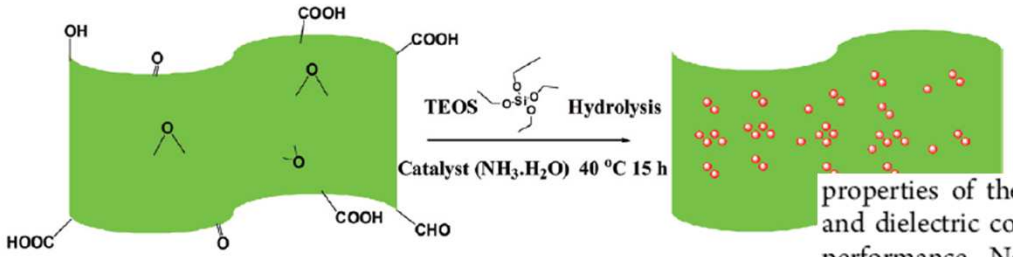

properties of the polarized particles, such as the conductivity and dielectric constant, have governing influences on their ER performance. Nevertheless, the electrical conductivity of the GO ($\sim 10^{-1}$ to 10^{-5} S/cm depending on the degree of oxidation) is still too high, which can cause an electric short in the ER measurement equipment. The addition of inorganic silica nanoparticles can help solve this problem. The ER properties can also be maximized by adjusting the optimum proportion of GO and tetraethyl orthosilicate (TEOS). Recently, silica nanoparticle-covered GO nanohybrids synthesized in a water−alcohol mixture were also reported regarding their superhydrophilic properties.[29]

Si-GO ≡ SiO_2-GrO

Making silica nanoparticle-covered graphene oxide nanohybrids as general building blocks for large-area superhydrophilic coatings†

Nanoscale, 2011, **3**, 519–528

Liang Kou and Chao Gao*

Received 18th August 2010, Accepted 15th October 2010
DOI: 10.1039/c0nr00609b

GrO-SiO_2 composites

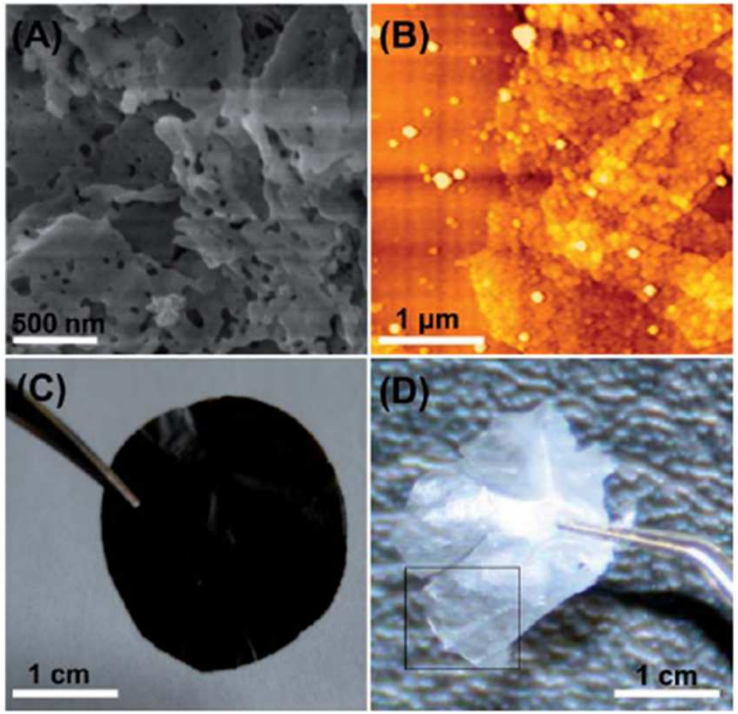

Fig. 6 SEM (A) and AFM (B) images of silica sheets obtained by calcining GO–SiO_2. Photographs of GO–SiO_2 paper (C) and the corresponding silica sheet paper (D) from burned GO–SiO_2.

semitransparent (labeled by a square frame) enabling the naked eye to see the rough background surface. As far as we know, it is the first time free-standing silica paper made of ultrathin silica nanosheets has been obtained; its special properties and applications are to be discovered.

Based on the high dense overlaying of silica nanoparticles, up to micro-scale silica sheets with thickness of *ca.* 8 nm were readily fabricated by burning GO–SiO_2 at 650 °C in air. Likewise, a centimeter-scale semitransparent film of silica nanosheets was prepared by calcining a GO–SiO_2 film. Interestingly, the

GrO-SiO_2 composites

Making silica nanoparticle-covered graphene oxide nanohybrids as general building blocks for large-area superhydrophilic coatings†

Nanoscale, 2011, **3**, 519–528

Liang Kou and Chao Gao*

Received 18th August 2010, Accepted 15th October 2010
DOI: 10.1039/c0nr00609b

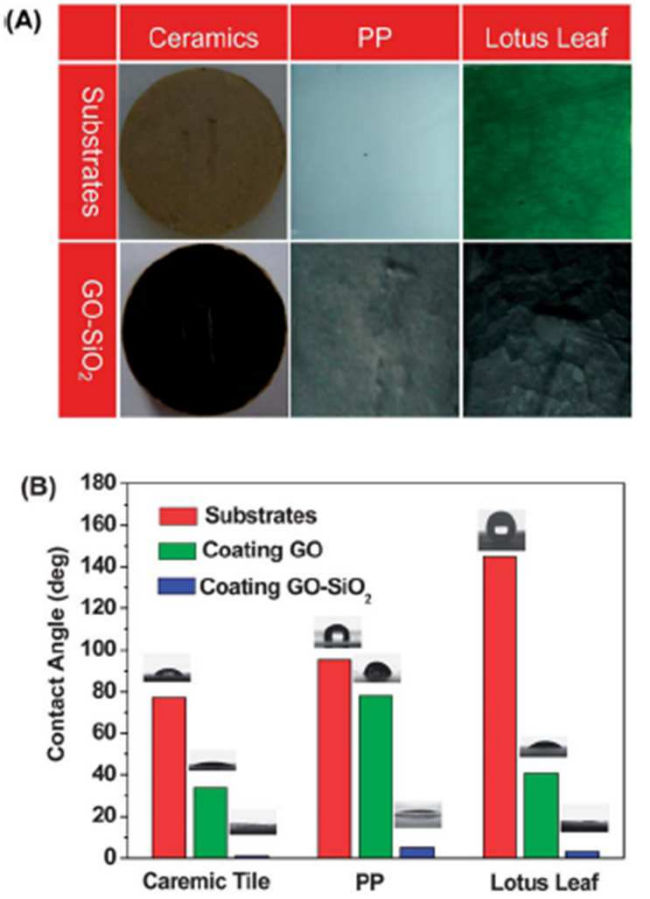

Fig. 7 (A) Photographs of blank substrates (top) and GO–SiO_2-coated substrates (bottom) of a ceramic tile, PP and a lotus leaf. (B) Water contact angles (WCAs) of blank, GO-coated and GO–SiO_2-coated substrates.

CONCLUSIONI

> Il grafene e' il primo materiale 2D

> I "derivati" del grafene sono di ampio interesse applicativo

> Le proprieta' fisiche dei materiali 2D sono di rilevante interesse teorico/sperimentale